doi: http://dx.doi.org/10.5016/1806-8774.2010v12p1

ARBS Annual Review of Biomedical Sciences

pdf freely available at http://arbs.biblioteca.unesp.br

2010;12:1-29

Electron Microscopic Radioautographic Studies on Macromolecular Synthesis in Mitochondria of Animal Cells in Aging

Tetsuji Nagata

Shinshu University School of Medicine and Shinshu Institute of Alternative Medicine and Welfare, JAPAN

Received: 25 October 2009; accepted 18 July 2010
Online on 09 September 2010

Abstract

Nagata T. Electron Microscopic Radioautographic Studies on Macromolecular Synthesis in Mitochondria of Animal Cells in Aging. ARBS Annu Rev Biomed Sci 2010;12:1-29. o study aging changes of intramitochondrial DNA, RNA, protein synthesis of mouse organs during the development and aging, 30 groups of developing and aging mice (3 individuals each), from fetal day 19 to postnatal newborn at day 1, 3, 9, 14 and adult at month 1, 2, 6, 12 to 24, were injected with either ^{3}H-thymidine, ^{3}H-uriidine, or ^{3}H-leucine, sacrificed 1 h later and liver, adrenal, lung and testis tissues observed by electron microscopic radioautography. Accordinlgy, numbers of mitochondria per cell profile area, numbers of labeled mitochondria and the mitochondrial labeling index labeled with ^{3}H-labeled precursors showing DNA, RNA, protein synthesis in these cells (hepatocytes, 3 zones of the adrenal cortices - zona glomerulosa, fasciculata and reticularis -, adrenal medullary cells, pulmonary cells and testis cells) were counted per cells and compared among the respective developing and aging groups. The numbers of mitochondria in these cells increased from fetal day 19 to postnatal month 1 and 2. However, the numbers of labeled mitochondria and the labeling indices of intramitochondrial DNA, RNA, protein syntheses incorporating the ^{3}H-labeled precursors in the described tissue cells increased from fetal day 19 to postnatal month 1 and decreased to month 24. These data support that the activity of intramitochnodrial DNA, RNA, protein syntheses in cells of these tissues increased and decreased by development and aging in mice. The intramitochondrial DNA, RNA and protein syntheses in some other organs were also reviewed and discussed.

Keywords: mice, liver, adrenal, DNA, RNA, protein synthesis, microscopic radioautography.

Table of Contents

Correspondence:
Tetsuji Nagata. Department of Anatomy and Cell Biology, Shinshu University School of Medicine, Matsumoto 390-8621, and Department of Anatomy, Shinshu Institute of Alternative Medicine and Welfare, Nagano 380-0816, Japan. Phone: +81-26-233-0555, FAX: +81-26-233-0591

E-mail: nagata@kowagakuen.ac.jp

1. Introduction

Intramitochondrial nucleic acid syntheses, both DNA and RNA, in mammalian and avian cells were first demonstrated morphologically by the present author and associates by means of electron microscopic radioautography with accurate localization in primary cultured cells of the livers and kidneys of mice, rats and chickens *in vitro* (Nagata et al., 1967) and then in some other established cell lines such as HeLa cells (Nagata, 1972a,b,c) or mitochondrial fractions prepared from *in vivo* cells (Nagata, 1974; Nagata et al., 1975, 1976). It was later commonly found in various cells and tissues not only *in vitro* obtained from various organs *in vivo* (Nagata, 1984; Nagata & Murata, 1977; Nagata et al., 1977), but also *in vivo* cells of various organs such as the salivary glands (Nagata et al., 2000), the liver (Nagata et al., 1979; 1982a,b; Nagata & Ma, 2005; Ma & Nagata, 1988; Ma et al., 1994), the pancreas (Nagata, 1992; Nagata et al., 1986), the trachea (Sun et al., 1997), the lung (Sun et al., 1995, 1997), the kidneys (Hanai & Nagata, 1994), the testis (Gao et al., 1994, 1995), the uterus (Yamada & Nagata, 1994), the adrenals (Ito & Nagata, 1996; Liang et al., 1999), the brains (Cui et al., 1996), the retina (Gunarso et al., 1996, 1997; Kong & Nagata, 1994) of chickens, mice and rats. The relationship between the intramitochondrial DNA synthesis and cell cycle was formerly studied and it was clarified that the intramitochondrial DNA synthesis was performed without nuclear involvement (Nagata, 1972a). However, the relationship between the DNA synthesis and the aging of individual animals has not yet been clarified. This paper deals with the relationship between the DNA synthesis and development in adrenal cortical cells of mice *in vivo* at various developmental stages from fetal day 19 to postnatal day 14 by means of electron microscopic radioautography as a part of serial studies on special cytochemistry (Nagata, 2001) and radioautographology (2002).

2. Radioautographic Procedures

2.1. Tissues and cells

We studied several kinds of cells in the liver, adrenal gland, lung and testis tissues of experimental

animals, mainly mice which were obtained from 30 groups of normal ddY strain mice, each consisting of 3 litter mates of both sexes, total 90, aged from embryonic day 19 to postnatal day 1, 3, 9 and 14 and month 1, 2, 6, 12 and 24. The embryonic age was based on observation of the vaginal plug of the female mice (vaginal plug = day 0). All the animals were housed under conventional conditions and bred with normal diet (mouse chow Clea EC2, Clea Co., Tokyo, Japan) with access to water ad libitum in our laboratory. They were administered with ^{3}H-thymidine or ^{3}H-uridine or ^{3}H-leucine, DNA, RNA and protein precursors, respectively, and the liver, adrenal and testis tissues were processed for light and electron microscopic radioautography (Nagata, 1996, 1997). All the procedures used in this study concerning the animal experiments were in accordance with the guidelines of the animal research committee of Shinshu University School of Medicine as well as the principles of laboratory animal care in NIH publication No. 86 -23 (revised 1985).

2.2. Radioautography

2.2.1. Light microscopic radioautography

All the animals were injected intraperitoneally with ^{3}H-thymidine (Amersham, England, specific activity 877 GBq/mM) or ^{3}H-uridine (Amersham, England, specific activity 1.11 TBq/mM) or ^{3}H-4,5-leucine (Amersham, England, specific acitivy 1002 GBq/mM) in saline, at 9 a.m., one hour before sacrifices. The dosage of injections was 370 KBq/gm body weight. The animals were perfused at 10 a.m., one hour after the injection, via the left ventricles of the hearts with 0.1 M cacodylate-buffered 2.5% glutaraldehyde under Nembutal (Abbott Laboratories, Chicago, ILL, USA) anesthesia. The right medical lobe of the liver, the superior lobe of the right lung, the right adrenal gland and the right testis were taken out, excised and 3 small tissue pieces from the respective organs (1 mm x 1 mm x 1 mm) were immersed in the same fixative at 4˚C for 1 h, followed by postfixation in 1% osmium tetroxide in the same buffer at 4˚C for 1 h, dehydrated in graded series of ethanol and acetone, and embedded in epoxy resin Epok 812 (Oken, Tokyo, Japan).

For light microscopic radioautography, thick sections (2.0µm) were cut in sequence on a Porter-Blum MT-2B ultramicrotome (Dupont-Sorvall, Newtown, MA, USA) using glass knives. The sections were collected on either collodion glass slides, coated with Konica NR-M2 radioautographic emulsion (Konica, Tokyo, Japan) by either dipping method (Nagata 1992, 1996, 1997, 2002). They were stored in dark boxes containing silica gel (desiccant) at 4˚C for exposure. After the exposure for several weeks, the specimens were processed for development in either SD-X1 developer at 20˚C (LM) in a water bath, rinsed in distilled water and dried in an oven at 37˚C overnight, stained with toluidine blue for 3 min and dried. The specimens were examined with an Olympus Vanox light microscope (Olympus Opt. Co., Tokyo, Japan).

2.2.2. Electron microscopic radioautography

For electron microscopic radioautography, semithin sections (0.2 µm) were cut in sequence on a Porter-Blum MT-2B ultramicrotome (Dupont-Sorvall, Newtown, MA, USA) using glass knives. The sections were collected on collodion coated copper grid meshes (VECO, Eerbeek, Netherlands), coated with Konica NR-H2 radioautographic emulsion (Konica, Tokyo, Japan) by a wire-loop method (Nagata, 1992, 1996, 1997, 2002). They were stored in dark boxes containing silica gel (desiccant) at 4˚C for exposure. After the exposure for several months, the specimens were processed for development in freshly prepared gold latensification solution for 30 s at 16˚C and then in fresh phenidon developer for 1 min at 16˚C in a water bath, rinsed in distilled water and dried in an oven at 37˚C overnight, stained with lead citrate solution for 3 min and coated with carbon. The electron microscopic radioautograms were examined in a JEOL JEM-4000EX electron microscope (JEOL, Tokyo, Japan) at accelerating voltages of 400 kV for observing thick specimens (Nagata, 1996, 1997, 2002).

2.2.3. Quantitative analysis of electron micrographs

For quantitative analysis of electron micrographs, twenty EM radioautograms showing cross sections of respective cell types from each group, based on the electron microscopic photographs taken after observation on at least 100 each cell type obtained from each animal, and at least 10 cells were analyzed to calculate the total number of mitochondria in each cell and the number of labeled mitochondria covered with silver grains by visual grain counting.

On the other hand, the number of silver grains in the same area size as a mitochondrion outside cells was also calculated in respective specimens as background fog, which resulted in less than 1 silver grain (0.03/mitochondrial area) almost zero. Therefore, the grain count in each specimen was not corrected with

background fog. From all the data thus obtained, the averages and standard deviations in respective aging groups were stochastically analyzed using variance and Student's t-test. The differences were considered to be significant at $P < 0.01$.

3. Special Radioautographology

3.1. The liver

3.1.1. Light microscopic radioautography

We studied the liver tissues of ddY strain mice at various ages from embryonic day 19 to postnatal 2 years. Observing light microscopic microscopic radioautograms labeled with ^{3}H-thymidine, the silver grains were found over the nuclei of some hepatocytes, demonstrating DNA synthesis (Fig. 1).

3.1.2. Electron microscopic radioautography

By electron microscopic radioautography, some nuclei and some mitochondria in hepatocytes in perinatal stages at embryonic day 19 (Fig. 2), postnatal day 1, 3, 9 and day 14 (Fig. 3) as well as young adult (Fig. 4) and senesecent animals (Fig. 5) were observed. However, those labeled hepatocytes were almost mononucleate cells (Figs. 2-5) and only a few binucleate cells were found among the mononucleate hepatocytes (Nagata & Ma, 2003). In the labeled hepatocytes (Figs. 1, 2, 3, 4, 5) the silver grains were mainly localized over the euchromatin of the nuclei and only a few or several silver grains were found over the mitochondria of these mononucleate hepatocytes (Nagata & Ma, 2005a; Nagata, 2007a,b,d,e). To the contrary, most hepatocytes were not labeled with any silver grains in their nuclei nor cytoplasm, showing no DNA synthesis even after labeling with 3H-thymidine in aged adult and senescent animals at postnatal month 1 (Fig. 4), 2, 6, 12 (Fig. 5) and month 24. On the other hand, labeled binucleate hepatocytes over their nuclei were very rarely found only at the perinatal stages from postnatal day 1, 3 (Fig. 6), 9 and 14 (Fig. 7) but not after postnatal month 1 to senescent stages up to month 12 or 24. Among many unlabeled hepatocytes, most mononucleate and binucleate hepatocytes were observed to be labeled with several silver grains over their mitochondria due to the incorporations of 3H-thymidine especially at the perinatal stages from embryonic day 19 to postnatal day 1, 3, 9 and 14 (Fig. 3). The localizations of silver grains over the mitochondria were mainly on the mitochondrial matrices but some grains over the mitochondrial membranes and cristae when observed by high power magnification (Fig. 3).

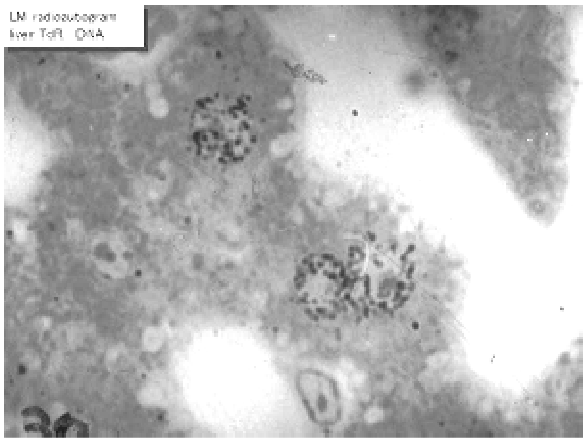

Figure 1: LM radioautogram of the liver of an adult mouse at postnatal month 1 labeled with ^{3}H-thymidine, demonstrating DNA synthesis in the two nuclei.

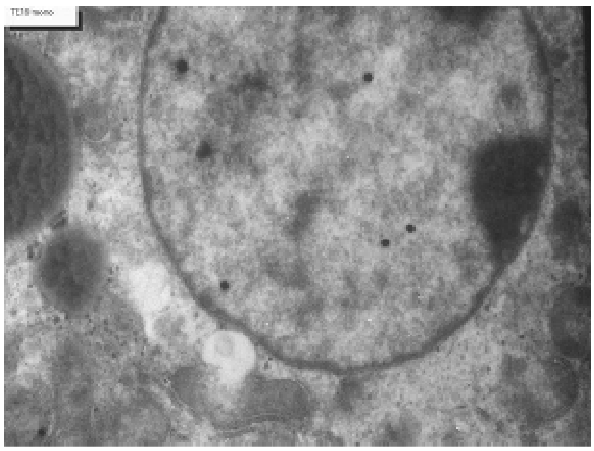

Figure 2: EM radioautogram of a mouse embryo liver aged at fetal day 19, labeled with ^{3}H-thymidine, demonstrating DNA synthesis of a mononucleate hepatocyte. Silver grains are localized over euchromatin of the nucleus as well as over a few mitochondria.

For preliminary quantitative analysis on the number of mitochondria in 10 mononucleate hepatocytes whose nuclei were labeled with silver grains and other 10 mononucleate hepatocytes whose nuclei were not labeled in each aging group injected with either ^{3}H-thymidine revealed that there was no significant difference between the number of mitochondria and the labeling indices in both types of hepatocytes ($P < 0.01$). Thus, the number of mitochondria and the labeling indices were calculated in both types of hepatocytes with labeled or unlabeled nuclei at respective aging stages. The results obtained from the number of mitochondria in mononucleate hepatocytes showed an increase from the prenatal day to postnatal day 14 (26.2-34.5/cell), then to postnatal month 1-6 (89.2-97.1/cell), reaching the maximum, then decreased to year 1-2 (80.4-85.7/cell) as is shown in Fig. 7 (top).

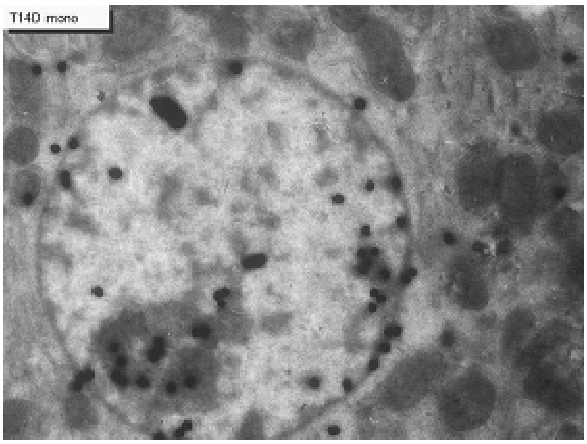

Figure 3: EM radioautogram of a mouse liver aged at postnatal day 14, labeled with ^{3}H-thymidine, demonstrating DNA synthesis of mononucleate hepatocyte. Silver grains are localized over euchromatin of the nucleus as well as over several mitochondria.

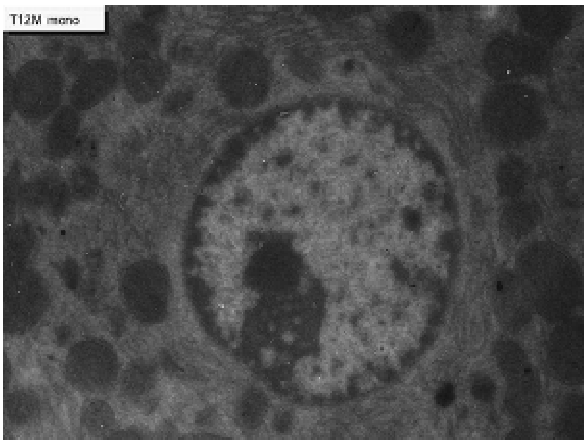

Figure 4: EM radioautogram of a senescent mouse aged at postnatal month 12, labeled with 3H-thymidine, demonstrating DNA synthesis of a mononucleiate hepatocyte. Silver grains are localized not over the nucleus but over a few mitochondria.

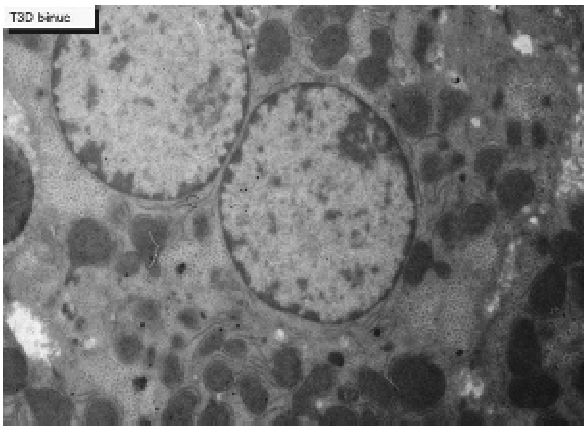

Figure 5: EM radioautogram of a newborn mouse aged at postnatal day 3, labeled with ^{3}H-thymidine, demonstrating DNA synthesis of a binucleate hepatocyte. Silver grains are localized not over the 2 nuclei but over a few mitochondria.

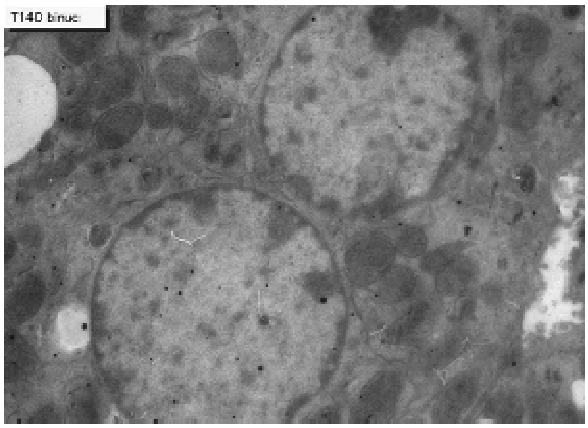

Figure 6: EM radioautogram of juvenile mouse aged at postnatal day 14, labeled with ^{3}H-thymidine, demonstrating DNA synthesis of a binucleate hepatocyte. Silver grains are localized over one of the 2 nuclei as well as over a few mitochondria.

3.1.2.1. Mitochondrial DNA synthesis in the liver

The results of visual counts on the number of mitochondria labeled with silver grains obtained from 10 mononucleate hepatocytes of each animal labeled with ^{3}H-thymidine demonstrating DNA synthesis in 7 aging groups at perinatal stages, prenatal embryo day 19, postnatal day 3, 9 and 14, month 1, 6 and 12, are plotted in Fig. 8 (middle). The labeling indices in respective aging stages were calculated from the number of labeled mitochondria (Fig. 8 middle) and the number of total mitochondria per cell (Fig. 8 top) which were plotted in Fig. 8 (bottom), respectively. The results showed that the numbers of labeled mitochondria with 3H-thymidine showing DNA synthesis increased from prenatal embryo day 19 (3.8/cell) to postnatal day 14 (6.2/cell), reaching the maximum, and then decreased to month 6 (3.7/cell) and again increased to year 1 (6.0/cell), while the labeling indices increased from prenatal day 19 (11.8%) to postnatal day 14 (16.9%), reaching the maximum, then decreased to month 6 (4.1%) and year 1 (6.4%) and year 2 (2.3%). The increase of the total number of mitochondria in mononucleate hepatocytes was stochastically significant ($P < 0.01$), while the changes of number of labeled mitochondria and labeling index in mononucleate hepatocytes were not significant ($P < 0.01$).

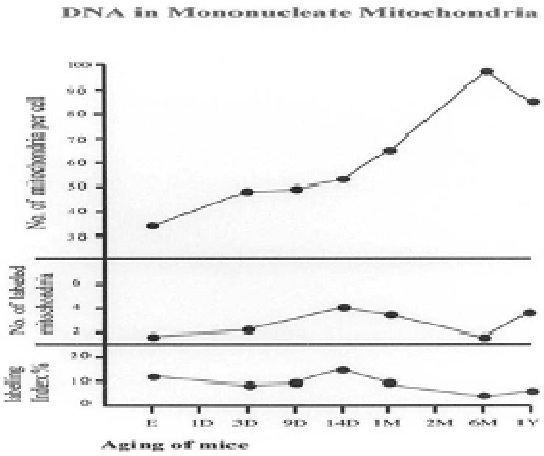

Figure 7: Transitional curves of the number of mitochondria per cell profile area (top), the number of labeled mitochondria per cell (middle) and the labeling index (bottom) of a monucleate hepatocyte in respective aging groups. The numbers and LI increased and decreased due to aging.

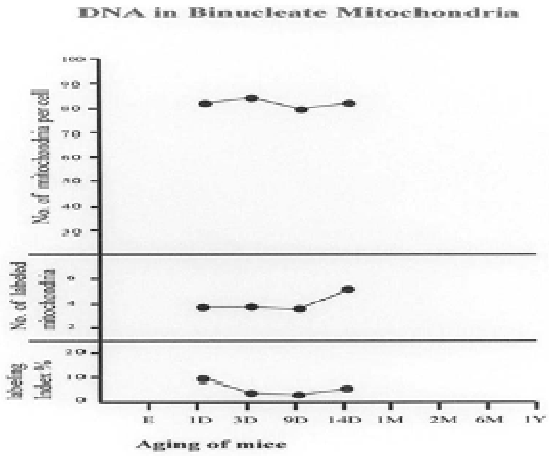

Figure 8: Transitional curves of the number of mitochondria per cell profile area (top), the number of labeled mitochondria per cell (middle) and the labeling index (bottom) of a binucleate hepatocyte in respective aging groups. The numbers and LI did not show any significant changes, but the number was much more than mononucleate cell at the same age.

As for the binucleate hepatocytes, on the other hand, because the appearances of binucleate hepatocytes showing silver grains in their nuclei demonstrating DNA synthesis were not so many in the adult and senescent stages from postnatal month 1 to 24, only binucleate cells at perinatal stages when reasonable numbers of labeled hepatocytes were found in respective groups were analyzed. The number of mitochondria in binucleate hepatocytes at postnatal day 1 to 14 kept around 80 (77-84/cell) which did not show such remarkable changes, neither increase nor decrease, as shown in mononucleate cells. Thus, the number of mitochondria per binucleate cell (Fig. 9 top), the number of labeled mitochondria per binucleate cell (Fig. 9 middle) and the labeling index of binucleate cell (Fig. 9 bottom) in 4 groups from postnatal day 1 to 14 were shown. The number of mitochondria and the number of labeled mitochondria were more in binucleate cells than mononucleate cells (Nagata, 2007a,b,d,e).

3.1.2.2. Mitochondrial RNA synthesis in the liver

On the other hand, observing light microscopic radioautograms labeled with ^{3}H-uridine, the silver grains were found over both the karyoplasm and cytoplasm of almost all the cells not only at the perinatal

stages from embryo day 19 to postnatal day 1, 3, 9, 14, but also at the adult and senescent stages from postnatal month 1 to 2, 6, 12 and 24 (Nagata, 2007a,b,d,e). By electron microscopic observation, silver grains were observed in most mononucleate hepatocytes in respective aging groups localizing not only over euchromatin and nucleoli in the nuclei but also over many cell organelles such as endoplasmic reticulum, ribosomes, and mitochondria as well as cytoplasmic matrices from perinatal stage at embryonic day 19 (Fig.10), postnatal day 1, 3 (Fig. 11), 9, 14 (Fig. 12), to adult and senescent stages at postnatal month 1 (Fig. 13), 2 (Fig. 14), 12 and 24. The silver grains were also observed in binucleate hepatocytes at postnatal day 1, 3, 9, 14, month 1, 2, 6 (Fig. 15), 12 and 24 (Fig. 16). The localizations of silver grains over the mitochondria were mainly on the mitochondrial matrices but a few over the mitochondrial membranes and cristae when observed by high power magnification (Fig. 12).

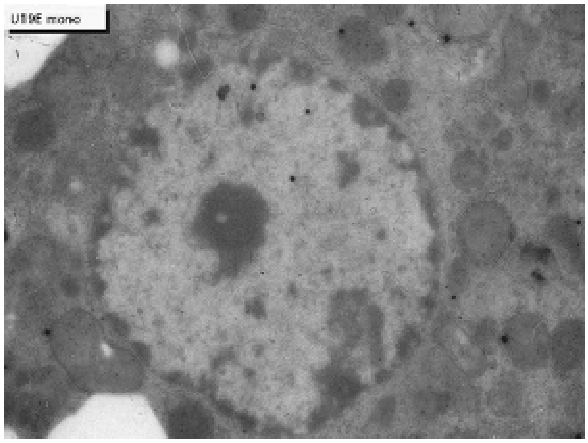

Figure 9: EMRAG of a mouse embryo liver at fetal day 19, labeled with ^{3}H-uridine, demonstrating RNA synthesis of a mononucleate hepatocyte. Several silver grains are localized over euchromatin of the nucleus as well as over several mitochondria.

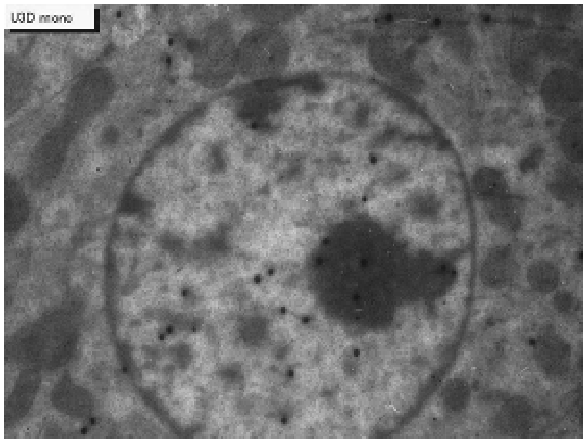

Figure 10: EMRAG of a newborn mouse liver at postnatal day 3, labeled with ^{3}H-uridine, demonstrating RNA synthesis of a mononucleate hepatocyte. Several silver grains are localized over euchromatin and nucleolus of the nucleus and over several mitochondria.

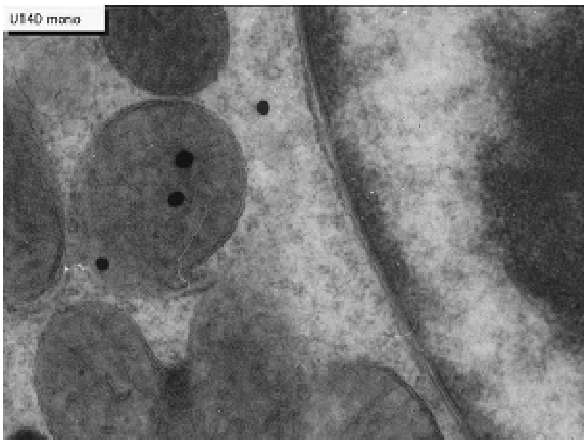

Figure 11: High power magnification EM radioautogram of a juvenile mouse liver at postnatal day 14, labeled with ^{3}H-uridine, demonstrating RNA synthesis. A few silver grains are localized over the mitochondrial matrix and the mitochondrial membrane of the mitochondrion at center.

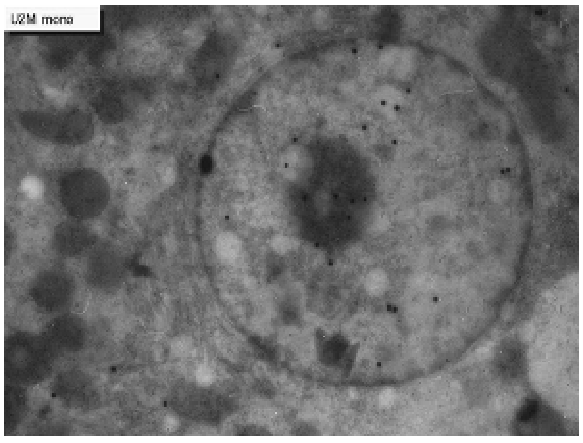

Figure 12: EMRAG of a senescent mouse liver at postnatal month 2, labeled with ^{3}H-uridine, demonstrating RNA synthesis of a mononucleate hepatocyte. Several silver grains are localized over euchromatin and nucleolus of the nucleus as well as over a few mitochondria showing less RNA synthesis than younger animals.

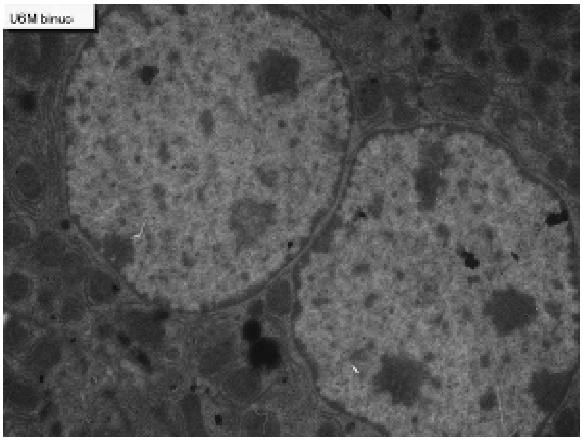

Figure 13: EMRAG of an adult mouse liver at postnatal month 6 labeled with ^{3}H-uridine, demonstrating RNA synthesis of a binucleate hepatocyte. Only a few silver grains are localized over the 2 nuclei and over a few mitochondria.

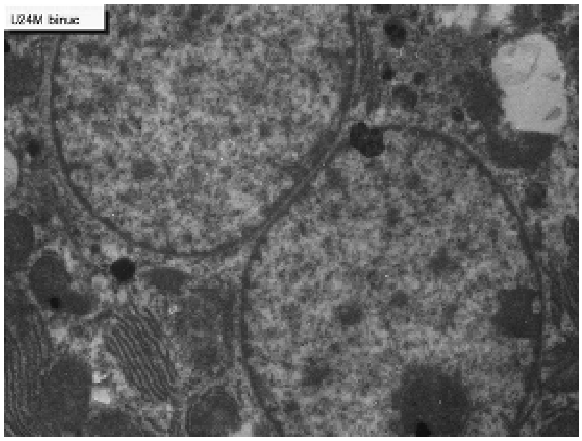

Figure 14: EMRAG of a senescent mouse liver at postnatal month 24, 2 years, labeled with ^{3}H-uridine, demonstrating RNA synthesis of a binucleate hepatocyte. Only a few silver grains are localized over the 2 nuclei and a few silver grains over a few mitochondria.

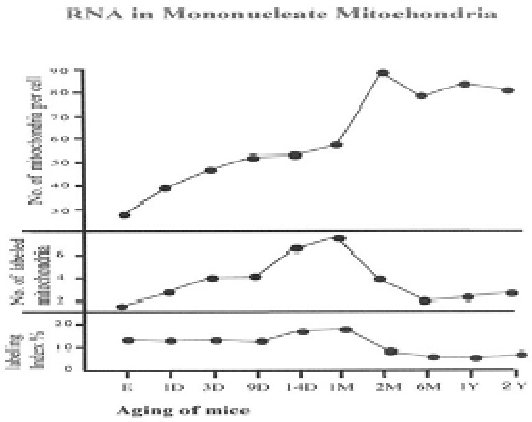

Figure 15: Transitional curves of the aging changes of the number of mitochondria per cell profile area (top), the number of labeled mitochondria per cell (middle) and the labeling index (bottom) of a monucleate hepatocyte in respective aging groups labeled with ^{3}H-uridine showing RNA synthesis. The number of labeled mitochondria and LI peaked at day 14

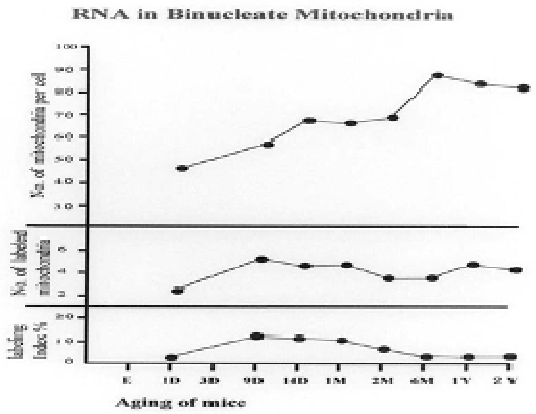

Figure 16: Transitional curves of the aging changes of the number of mitochondria per cell profile area (top), the number of labeled mitochondria per cell (middle) and the labeling index (bottom) of binucleate hepatocyte in respective aging groups labeled with ^{3}H-uridine showing RNA synthesis.

As the results, it was found that almost all the hepatocytes were labeled with silver grains showing RNA synthesis in their nuclei and mitochondria (Nagata & Ma, 2005b,c). Preliminary quantitative analysis on the number of mitochondria in 10 mononucleate hepatocytes whose nuclei were intensely labeled with many silver grains (more than 10 per nucleus) and other 10 mononucleate hepatocytes whose nuclei were not so intensely labeled (number of silver grains less than 9) in each aging group revealed that there was no significant difference between the number of mitochondria, number of labeled mitochondria and the labeling indices in both types of hepatocytes ($P < 0.01$). Thus, the number of mitochondria and the labeling indices were calculated in 10 hepatocytes selected at random in each animal in respective aging stages regardless whether their nuclei were very intensely labeled or not. The results obtained from the number of mitochondria in mononucleate hepatocytes per cellular profile area showed an increase from the prenatal day (mean ± standard deviation 26.2± /cell) to postnatal day 1 to day 14 (38.4-51.7/cell), then to postnatal

month 1-2 (53.7-89.2/cell), reaching the maximum, then decreased to year 1-2 (83.7-80.4/cell) as is shown in Fig. 16 (top) and the increase was stochastically significant ($P < 0.01$). The results of visual grain counts on the number of mitochondria labeled with silver grains obtained from 10 mononucleate hepatocytes of each animal labeled with 3H-uridine demonstrating RNA synthesis in 10 aging groups at perinatal stages, prenatal embryo day 19, postnatal day 1, 3, 9 and 14, month 1, 6 and year 1 and 2, are plotted in Fig. 17 (middle). The labeling indices in respective aging stages were calculated from the number of labeled mitochondria (Fig. 17, middle) and the number of total mitochondria per cellular profile area (Fig. 17, top) which were plotted in Fig. 16 (bottom), respectively. The results showed that the numbers of labeled mitochondria with ^{3}H-uridine showing RNA synthesis increased from prenatal embryo day 19 (3.3/cell) to postnatal month 1 (9.2/cell), reaching the maximum, and then decreased to month 6 (3.5/cell) and again increased to year 1 (4.0/cell) and year 2 (4.3/cell), while the labeling indices increased from prenatal day 19 (12.4%) to postnatal month 1 (16.7%), reaching the maximum, then decreased to year 1 (4.8%) and year 2 (5.3%). Stochastical analysis revealed that the increases and decreases of the number of labeled mitochondria from the perinatal stage to the adult and senescent stage were significant in contrast that the increases and decreases of the labeling indices were not significant ($P < 0.01$). As for the binucleate hepatocytes, on the other hand, because the appearances of binucleate hepatocytes were not so many in the embryonic stage, only several binucleate cells (5-8 at least) at respective stages when enough numbers of binucleate cells available from postnatal day 1 to year 2 were analyzed.

The results were shown in Fig. 18. The results of visual counts on the number of mitochondria labeled with silver grains obtained from several (5 to 8) binucleate hepatocytes labeled with 3H-uridine demonstrating RNA synthesis in 8 aging groups at perinatal stages, postnatal day 1, 9, 14, and month 1, 2, 6, and year 1 and 2, are plotted in Fig. 16 (middle) and the labeling indices in respective aging stages were calculated from the number of labeled mitochondria (Fig. 16, middle) and the number of total mitochondria per cellular profile area (Fig. 18, top) which were plotted in Fig. 16 (bottom), respectively. The results showed that the number of labeled mitochondria increased from postnatal day 1 (2.3/cell) to day 9 (5.2/cell) and remained almost constant around 4-5, but the labeling indices increased from postnatal day 1 (2.1%) to postnatal day 9 (13.6%), remained almost constant around 13% (12.5-13.6%) from postnatal day 9 to month 1, then decreased to month 2 (6.1%) to month 6 (3.9%), and slightly increased to year 1 (6.3%) and 2 (5.3%). The increases and decreases of the number of labeled mitochondria and the labeling indices in binucleate hepatocytes were stochastically not significant ($P < 0.01$).

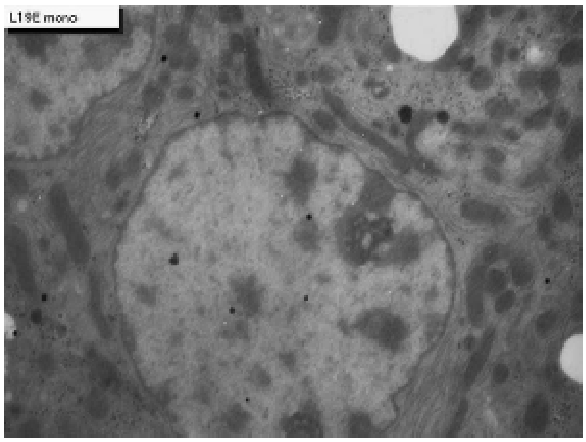

Figure 17: EMRAG of a mouse embryo liver at fetal day 19, labeled with ^{3}H-leucine, demonstrating protein synthesis of a mononucleate hepatocyte. Several silver grains are localized over euchromatin of the nucleus and over several mitochondria.

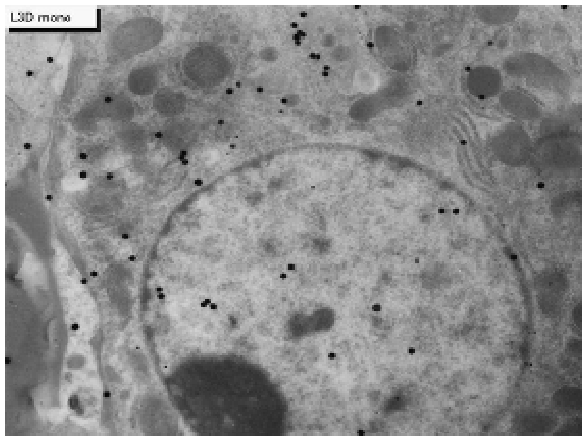

Figure 18: EMRAG of a newborn mouse liver at postnatal day 3, labeled with ^{3}H-leucine, demonstrating protein synthesis of a mononucleate hepatocyte. Several silver grains are localized over euchromatin of the nucleus and over several mitochondria.

3.1.2.3. Mitochondrial protein synthesis in the liver

When the animals were injected with ^{3}H-leucine, it was found that almost all the hepatocytes, from embryonic day 19, postnatal day 1, 3 (Fig. 19), 9, 14 (Fig. 20), to adult and senescent stages at postnatal month 1, 2 (Fig. 21), 12 and 24 (Fig. 22). The silver grains were also observed in binucleate hepatocytes at postnatal day 1, 3 (Fig. 23), 9, 14 (Fig. 24), month 1, 2, 6, 12 (Fig. 25) and 24 (Nagata, 2007c,f). The localizations of silver grains observed over the mitochondria were mainly on the mitochondrial matrices but a few over their nuclei, cytoplasmic matrix, endoplasmic reticulum, ribosomes, Golgi apparatus and mitochondria (Nagata, 2006). In the mitochondria the silver grains were localized over the mitochondrial membranes and cristae when observed by high power magnification (Fig. 19). Preliminary quantitative analysis on the number of mitochondria in 20 mononucleate hepatocytes whose nuclei were intensely labeled with many silver grains (more than 10 per nucleus) and other 20 mononucleate hepatocytes whose nuclei were not so intensely labeled (number of silver grains less than 9) in each aging group revealed that there was no significant difference between the number of mitochondria, number of labeled mitochondria and the labeling indices in both types of hepatocytes ($P < 0.01$).

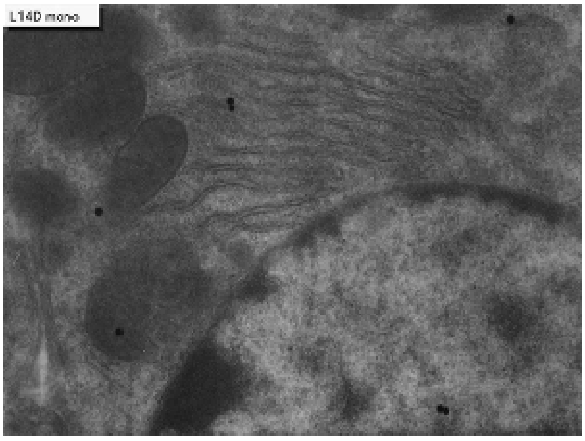

Figure 19: High power magnification radioautogram of a juvenile mouse liver at postnatal day 14, labeled with 3H-leucine, demonstrating protein synthesis. A few silver grains are localized over the mitochondrial matrix of the 2 mitochondria at left.

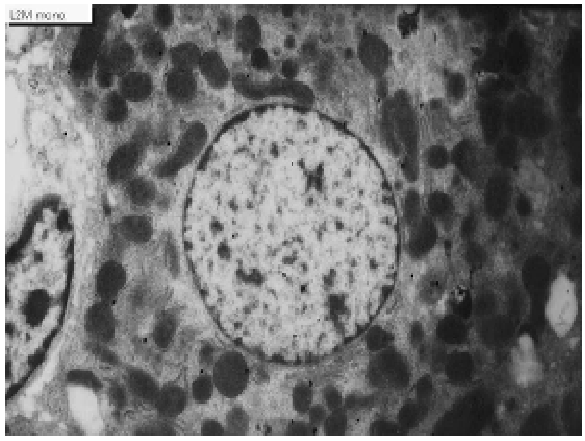

Figure 20: EMRAG of an adult mouse liver at postnatal month 2, labeled with ^{3}H-leucine, demonstrating protein synthesis of a mononucleate hepatocyte. Several silver grains are localized over the nucleus and over several mitochondria.

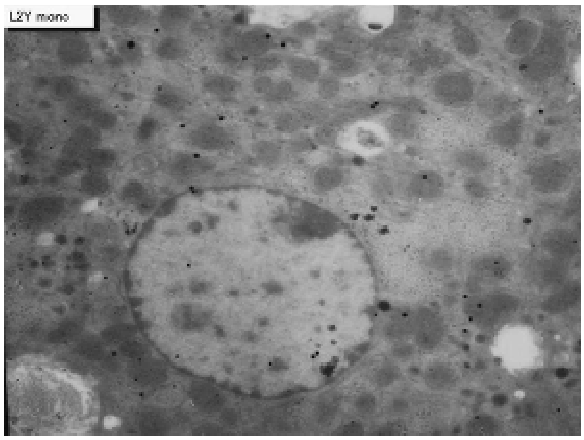

Figure 21: EMRAG of a senescent mouse liver at postnatal month 24, 2 years, labeled with ^{3}H-leucine, demonstrating protein synthesis of a mononucleate hepatocyte. Several silver grains are localized over euchromatin of the nucleus as well as over a few mitochondria showing less protein than younger animals.

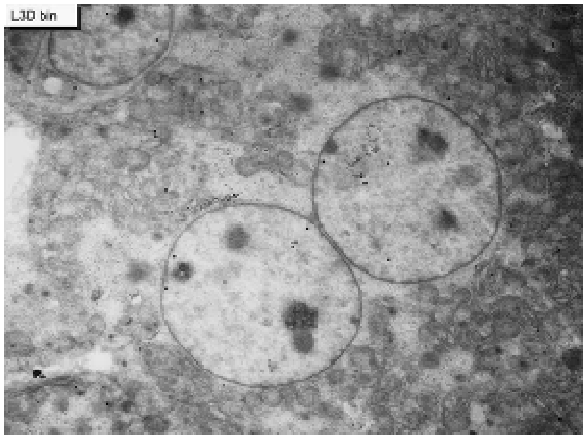

Figure 22: Next slide shows an EMRAG of mouse liver at postnatal day 3, a newborn mouse, labeled with ^{3}H-leucine, demonstrating protein synthesis of a binucleate hepatocyte. Only a few silver grains are localized over the 2 nuclei and over a few mitochondria.

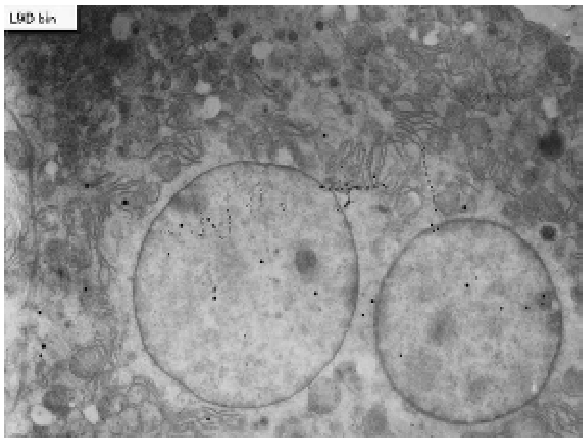

Figure 23: EMRAG of mouse a juvenile mouse liver at postnatal day 9, labeled with ^{3}H-leucine, demonstrating protein synthesis of a binucleate hepatocyte. Only a few silver grains are localized over the 2 nuclei and over a few mitochondria.

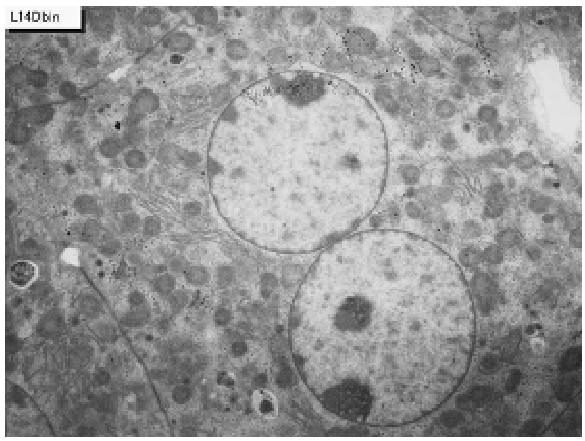

Figure 24: EMRAG of a juvenile mouse liver at postnatal day 14, labeled with ^{3}H-leucine, demonstrating protein synthesis of a binucleate hepatocyte. Only a few silver grains are localized over the 2 nuclei and over a few mitochondria.

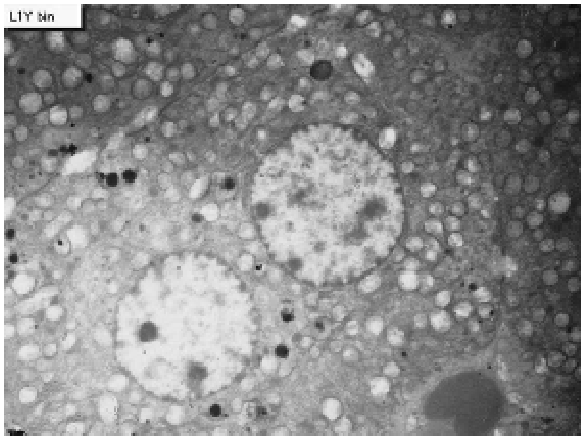

Figure 25: EMRAG of senescent mouse liver at postnatal month 12, year 1, labeled with ^{3}H-leucine, demonstrating protein synthesis of a binucleate hepatocyte. Only a few silver grains are localized over the 2 nuclei and over a few mitochondria.

On the other hand, the numbers of mitochondria, the numbers of labeled mitochondria and the labeling indices were calculated in 10 binucleate hepatocytes selected at random in each animal in respective aging stages, regardless whether their nuclei were very intensely labeled or not, except the prenatal stage at embryonic day 19, because no binucleate cell was found at this stage. Thus, the numbers of mitochondria, the numbers of labeled mitochondria and the labeling indices were calculated in 20 hepatocytes selected at random in each animal in respective aging stages regardless whether their nuclei were very intensely labeled or not. The results obtained from the total numbers of mitochondria in mononucleate hepatocytes showed an increase from the prenatal day (34.5/cell) to postnatal days 1 (44.6/ cell), 3 (45.8/cell), 9 (43.6/cell), 14 (48.5/cell), to postnatal months 1 (51.5/cell), 2 (52.3/cell), reaching the maximum at month 6 (60.7/cell), then decreased to years 1 (54.2/cell) and 2 (51.2/cell) as shown in Fig. 25 (upper left). The increase and decrease were stochastically significant ($P < 0.01$). The results obtained from visual counting on the numbers of mitochondria labeled with silver grains from 20 mononucleate hepatocytes of each animal labeled with 3H-leucine demonstrating protein synthesis in 10 aging groups at perinatal stages, prenatal embryo day 19, postnatal day 1, 3, 9 and 14, month 1, 2, 6 and year 1 and 2, are

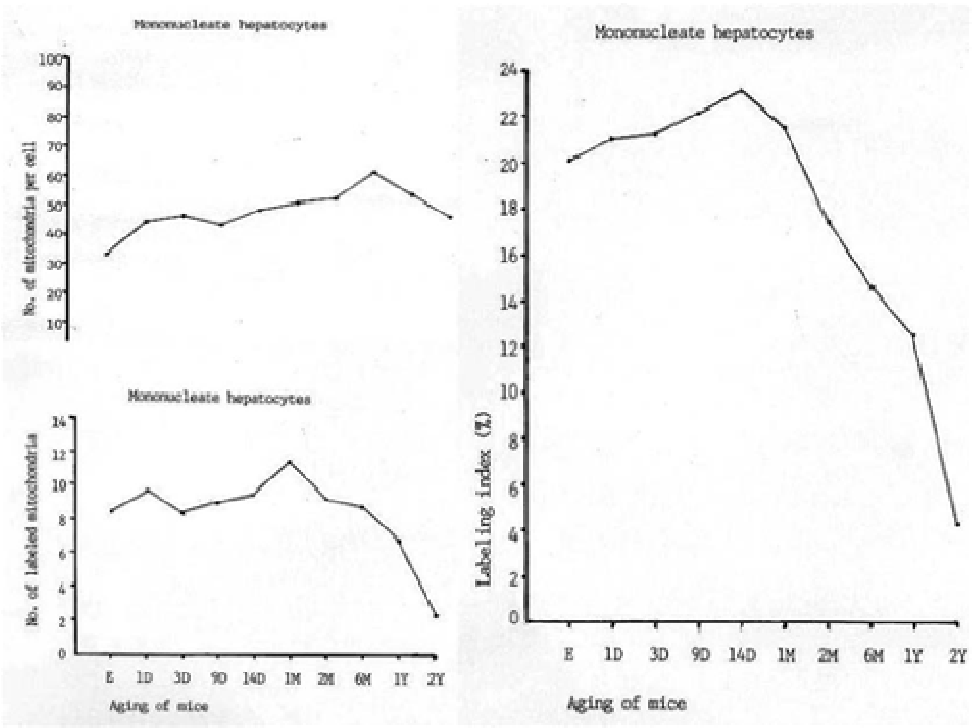

Figure 26: Transitional curves of the aging changes of mononucleate hepatocyte mitochondria labeled with ^{3}H-leucine showing protein synthesis. The upper left curve shows number of mitochondria per cell showing an increase and decrease due to aging, the lower left curve shows number of labeled mitochondria per cell, which showed an increase and decrease, and the right curve shows labeling index which also showed an increase and decrease with aging.

plotted in Fig. 26 (lower left). The labeling indices in respective aging stages were calculated from the numbers of labeled mitochondria and the numbers of total mitochondria per cell which were plotted in Fig. 26 (right). The results showed that the numbers of labeled mitochondria with 3H-leucine showing protein synthesis increased from prenatal embryo day 19 (8.3/cell) to postnatal days 1 (9.6/cell), 3 (8.1/cell), 9 (8.9/cell), 14 (9.5/cell), and month 1 (11.2/cell), reaching the maximum, and then decreased to months 2 (9.1/cell), 6 (8.8/cell) to years 1 (6.7/cell) and 2 (2.2/cell), while the labeling indices increased from prenatal day 19 (20.1%) to postnatal days 1 (21.2%), 3 (21.6%), 9 (22.2%), 14 (23.1%), reaching the maximum, then decreased to month 1 (21.7%), 2 (17.4%), 6 (14.6%), and years 1 (12.4%) and 2 (4.4%). Stochastical analysis revealed that the increases and decreases of the numbers of labeled mitochondria as well as the labeling indices from the perinatal stage to the adult and senescent stages were significant ($P < 0.01$).

On the other hand, the results obtained from the numbers of mitochondria in binucleate hepatocytes showed an increase from the postnatal days 1 (66.2/cell), to 3 (66.4/cell), 14 (81.8/cell), to postnatal months 1 (89.9/cell), 2 (95.1/cell), and 6 (102.1), reaching the maximum at month 12 (128.0/cell), then decreased to years 2 (93.9/cell) as shown in Fig. 27 (upper left). The increase and decrease were stochastically significant ($P < 0.01$). The results obtained from visual counting on the numbers of mitochondria labeled with silver grains from 10 binucleate hepatocytes of each animal labeled with 3H-leucine demonstrating protein synthesis in 10 aging groups at postnatal day 1, 3, and 14, month 1, 6 and year 1 and 2, are plotted in Fig. 27 (lower left). The labeling indices in respective aging stages were calculated from the numbers of labeled mitochondria and the numbers of total mitochondria per cell which were plotted in Fig. 27 (right). The results showed that the numbers of labeled mitochondria with ^{3}H-leucine showing protein synthesis increased from postnatal day 1 (7.3/cell) to day 3 (6.8/cell), 14 (10.2/cell), and month 1 (15.0/cell), 2 (15.9/cell), reaching the maximum at month 6 (19.6/cell), then decreased to year 1 (8.3/cell) and 2 (5.1/cell), while the labeling indices increased from postnatal day 1 (11.8%) to 3 (10.2%), 14 (12.5%), month 1 (18.3%) and 2 (18.7%), reaching the maximum at month 6 (19.2%), then decreased to year 1 (6.4%) and 2 (5.5%). Stochastical analysis revealed that the increases and decreases of the numbers of labeled mitochondria as well as the labeling indices from the newborn stage to the adult and senescent stages were significant ($P < 0.01$) (Nagata, 2007c).

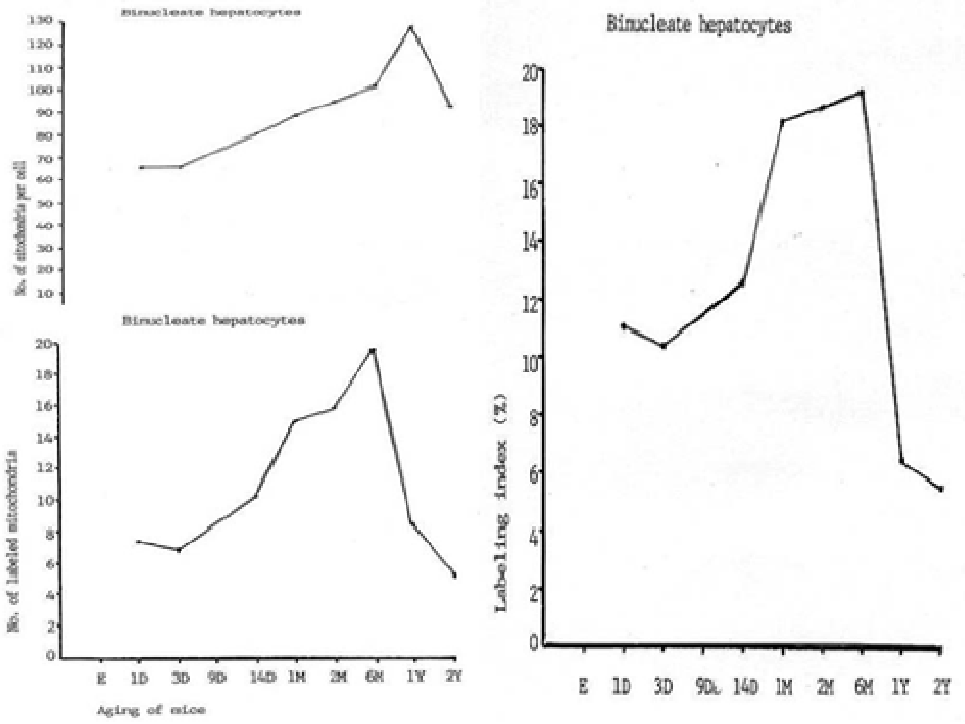

Figure 27: Transitional curves of the aging changes of binucleate hepatocyte mitochondria labeled with ^{3}H-leucine showing protein synthesis. The upper left curve shows number of mitochondria per cell, which had much more mitochondria than mononucleate cell and showed an increase and decrease due to aging, the lower left shows number of labeled mitochondria per cell, which showed an increase and decrease, and the right shows labeling index which also showed an increase and decrease with

3.2. The adrenal gland

The adrenal gland of a mouse consists of both the adrenal cortex and the adrenal medulla. The adrenal cortex of a mouse hsitologically consists of 3 layers, i. e., zona glomerulosa, zona fasciculate and zona reticularis. The adrenal medulla consists of 2 cell types, i. e., adrenalin cells and noradrenalin cells (Ito & Nagata, 1996; Liang et al., 1999).

3.2.1. Adrenal cortex

We studied the adrenal tissues at various ages from embryo to postnatal 2 years (Ito & Nagata, 1996; Liang et al., 1999). The adrenal tissues obtained from ddY strain mice at various ages from embryo day 19 to postnatal day 30, consisted of the adrenal cortex and the adrenal medulla. The former consited of 3 layers, developing gradually with aging as observed by light microscopy. At embryonic day 19 and postnatal day 1, the adreno-cortical cells were composed mainly of polygonal cells, while the specific orientation of the 3 layers, zona glomerulosa, zona fasciculata and zona reticularis, was not yet well established. At postnatal day 3, orientation of 3 layers, especially the zona glomerulosa became evident. At postnatal day 9 and 14, the specific structure of 3 layers was completely formed and the arrangements of the cells in respective layer became typical especially at day 14 and month 1 (Fig. 28). Observing the ultrastructure of the adreno-cortical cells by electron microscopy, cell organelles including mitochondria were not so well developed at perinatal and early postnatal stages from embryonic day 19 to postnatal day 9. However, these cell organelles, mitochondria, endoplasmic reticulum, Golgi apparatus, appeared well developed similarly to the adult stages at postnatal day 14. The zona glomerulosa (Figs. 29, 32, 35, 38) is the thinnest layer found at the outer zone, covered by the capsule, consisted of closely packed groups of columnar or pyramidal cells forming arcades of cell columns. The cells contained many spherical mitochondria and well developed smooth surfaced endoplasmic reticulum but a compact Golgi apparatus in day 14 animals. The zona fasciculata (Figs. 30, 33, 36, 39) was the thickest layer, consisted of polygonal cells which were larger than the glomerulosa cells, arranged in long cords disposed radially to the medulla

containing many lipid droplets (Figs. 33, 36, 39). The mitochondria were less numerous and were more variable in size and shape than those of the glomeruloza cells, while the smooth surfaced endoplasmic reticulum were more developed and the Golgi apparatus was larger than the glomerulosa. In the zona reticularis (Figs. 31, 34, 37, 40), the parallel arrangement of cell cords were anastomosed showing networks continued to the medullar cells. The mitochondria were less numerous and were more variable in size and shape than those of the glomeruloza cells like the fasciculata cells, as well as the smooth surfaced endoplasmic reticulum were developed and the Golgi apparatus was large like the fasciculata cells. However, the structure of the adrenal cortex tissues showed changes due to development and aging at respective developmental stages.

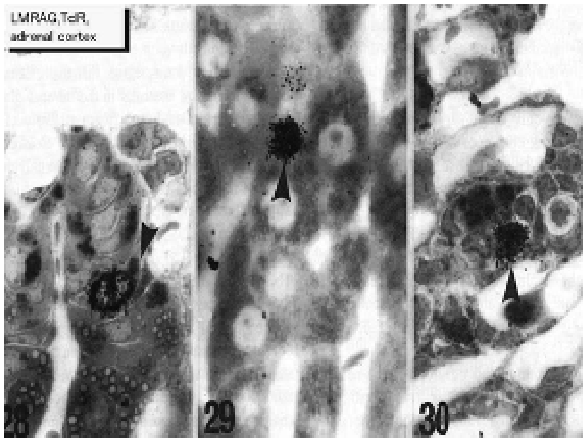

Figure 28: LM radioautograms of a young mouse adrenal cortex, zona glomerulosa (left), fasciculata (center), and reticularis (right), labeled with ^{3}H-thymidine, demonstrating DNA synthesis of adreno-cortical cells. Silver grains are localized over the nuclei in each zone (arrows).

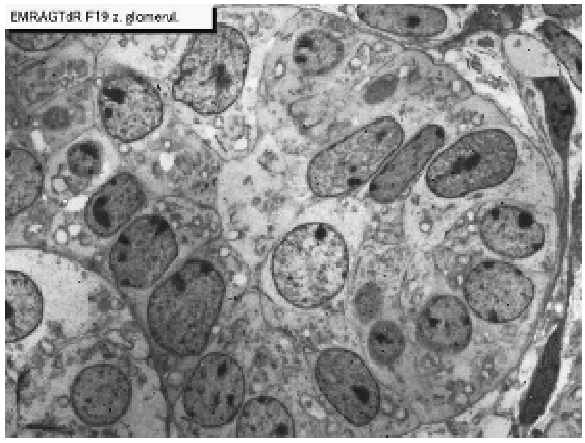

Figure 29: EM radioautogram of a mouse embryo adrenal gland at fetal day 19, labeled with 3H-thymidine, demonstrating DNA synthesis of adreno-cortical cells at zona glomerulosa. Silver grains are localized over euchromatin of the nuclei as well as over a few mitochondria.

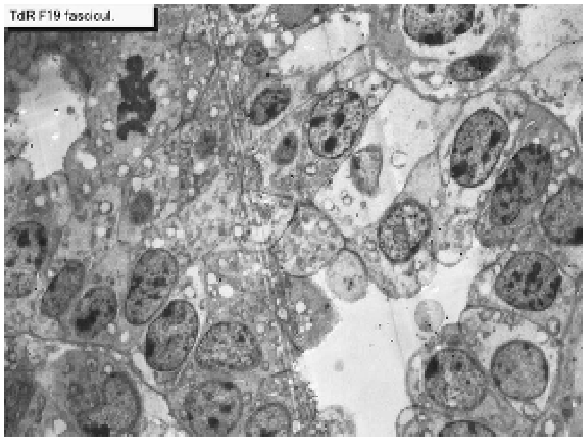

Figure 30: EMRAG of a mouse embryo adrenal gland at fetal day 19, labeled with ^{3}H-thymidine, demonstrating DNA synthesis of adreno-cortical cells at zona fasciculata. Silver grains are localized over euchromatin of the nuclei as well as over a few mitochondria.

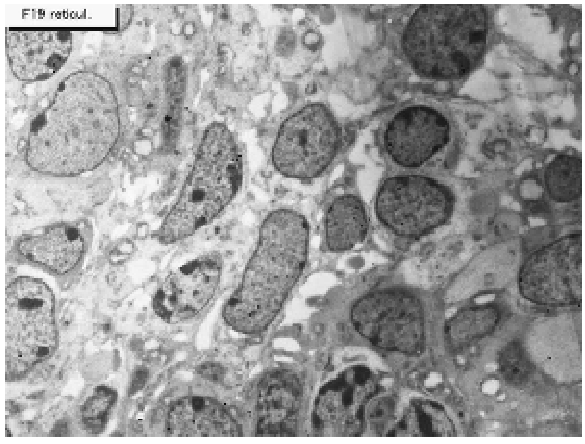

Figure 31: EMRAG of a mouse embryo adrenal gland at fetal day 19, labeled with ^{3}H-thymidine, demonstrating DNA synthesis of adreno-cortical cells at zona reticularis. Silver grains are localized over euchromatin of the nuclei as well as over a few mitochondria.

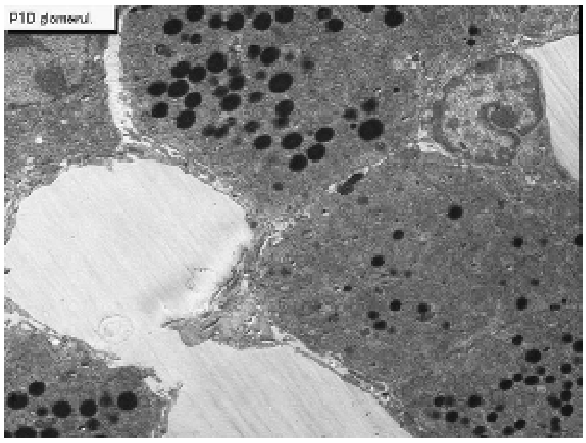

Figure 32: EMRAG of mouse adrenal gland at postnatal day 1, labeled with ^{3}H-thymidine, demonstrating DNA synthesis of adreno-cortical cells at zona glomerulosa.

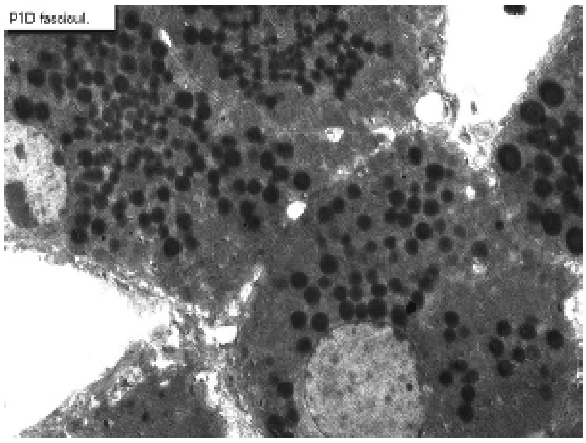

Figure 33: EMRAG of a newborn mouse adrenal gland at postnatal day 1, labeled with ^{3}H-thymidine, demonstrating DNA synthesis of adreno-cortical cells at zona fasciculata.

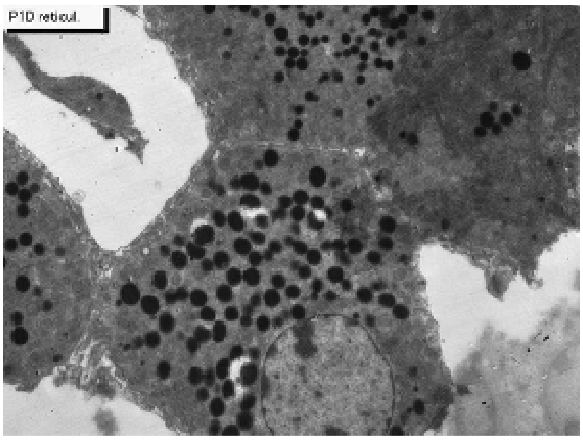

Figure 34: EMRAG of newborn mouse adrenal gland at postnatal day 1, labeled with ^{3}H-thymidine, demonstrating DNA synthesis of adreno-cortical cells at zona reticularis.

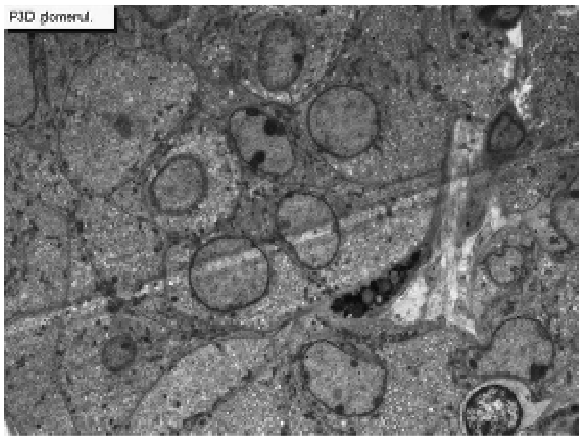

Figure 35: EMRAG of a newborn mouse adrenal gland at postnatal day 3, labeled with ^{3}H-thymidine, demonstrating DNA synthesis of adreno-cortical cells at zona glomerulosa.

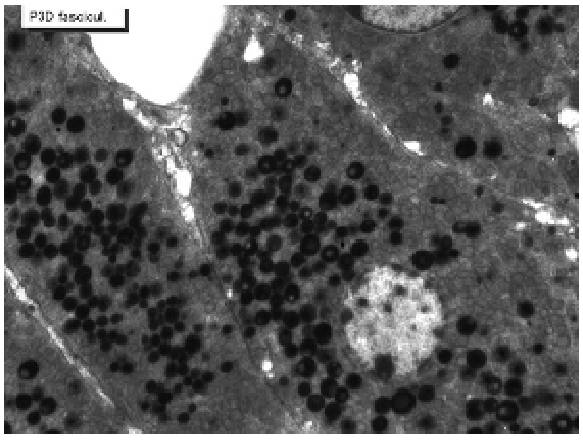

Figure 36: EMRAG of a newborn mouse adrenal gland at postnatal day 3, labeled with ^{3}H-thymidine, demonstrating DNA synthesis of adreno-cortical cells at zona fasciculata.

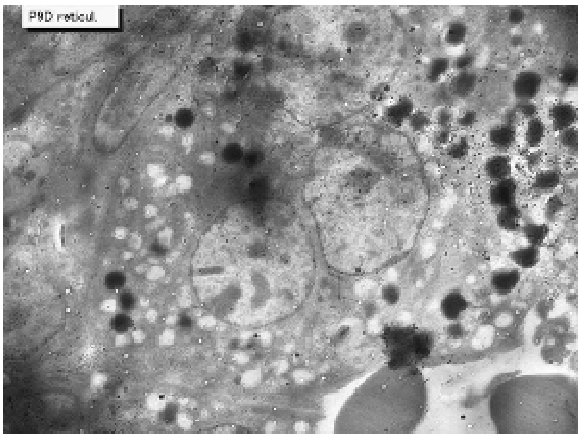

Figure 37: EMRAG of a juvenile mouse adrenal gland at postnatal day 9, labeled with ^{3}H-thymidine, demonstrating DNA synthesis of adreno-cortical cells at zona reticularis.

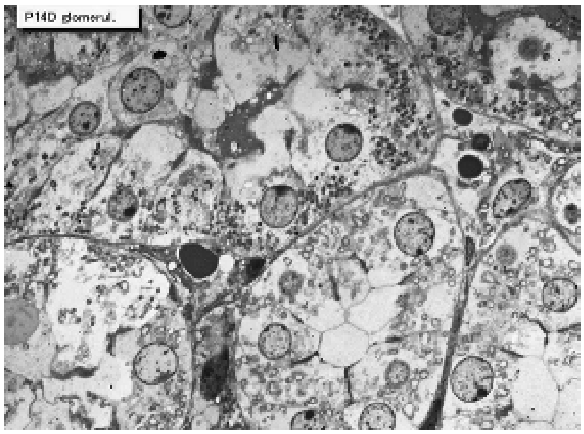

Figure 38: EMRAG of a juvenile mouse adrenal gland at postnatal day 14, labeled with ^{3}H-thymidine, demonstrating DNA synthesis of adreno-cortical cells at zona glomerulosa.

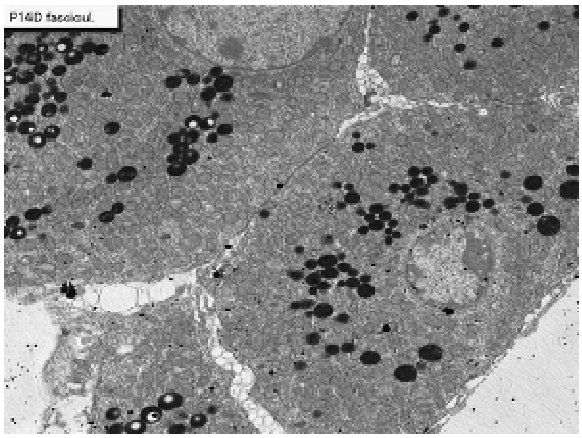

Figure 39: EMRAG of a juvenile mouse adrenal gland at postnatal day 14, labeled with ^{3}H-thymidine, demonstrating DNA synthesis of adreno-cortical cells at zona fasciculata.

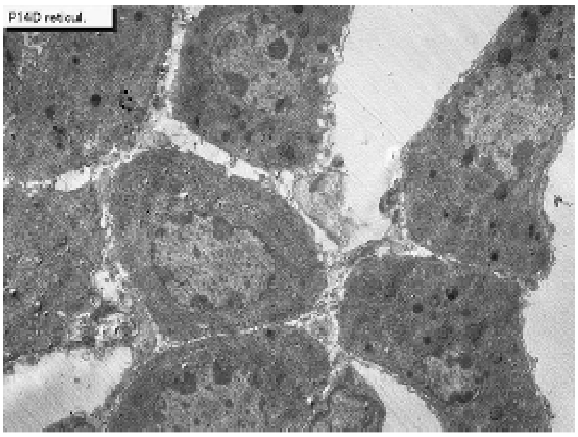

Figure 40: EMRAG of juvenile mouse adrenal gland at postnatal day 14, labeled with ^{3}H-thymidine, demonstrating DNA synthesis of adreno-cortical cells at at zona reticularis.

3.2.1.1. DNA synthesis in the adreno-cortical cells

Observing EM radioautograms, the silver grains were found over the nuclei of some adreno-cortical cells labeled with ^{3}H-thymidine, demonstrating DNA synthesis mainly in perinatal stages at embryonic day 19 (Figs. 29, 30, 31), postnatal day 1 (Figs. 32, 33, 34) and day 3 (Figs. 35, 36), while less at day 9 (Fig. 37), and day 14 (Figs. 38, 39, 40) (Ito & Nagata, 1996).

However, those labeled cells were found in all the 3 layers, the zona glomerulosa (Figs. 29, 32, 35, 38), the zona fasciculata (Figs. 30, 33, 36, 39) and the zona reticularis (Figs. 31, 34, 36, 37, 40), at respective aging stages. In the labeled adreno-cortical cells in 3 layers the silver grains were mainly localized over the euchromatin of the nuclei and only a few or several silver grains were found over the mitochondria of these cells. To the contrary, most adreno-cortical cells were not labeled with any silver grains in their nuclei nor cytoplasm, showing no DNA synthesis even after labeling with 3H-thymidine. Among many unlabeled adreno-cortical cells, most cells in the 3 layers were observed to be labeled with several silver grains over their mitochondria due to the incorporations of 3H-thymidine especially at the perinatal stages from embryonic day 19 (Fig. 29, 30, 31) to postnatal day 1 (Fig. 32, 33, 34), day 3 (Fig. 35, 36), day 9 (Fig. 37) and 14 (Fig. 38, 39, 40). The localizations of silver grains over the mitochondria were mainly on the mitochondrial matrices when observed by high power magnification (Fig. 39).

3.2.1.1.1. Quantitative analysis on the DNA synthesis of adreno-cortical cells

3.2.1.1.1.1. Number of mitochondria per cell

Preliminary quantitative analysis on the number of mitochondria in 10 adreno-cortical cells whose nuclei were labeled with silver grains and other 10 cells whose nuclei were not labeled in each aging group revealed that there was no significant difference between the number of mitochondria and the labeling indices ($P < 0.01$). Thus, the number of mitochondria and the labeling indices were calculated regardless whether their nuclei were labeled or not. The results obtained from the number of mitochondria in adreno-cortical cells in the 3 layers of respective animals in 5 aging groups at perinatal stages, prenatal embryo day 19, postnatal day 1, 3, 9 and 14, showed an gradual increase from the prenatal day 19 (glomerulosa 12.5, fasciculata 14.9, reticularis 15/2/cell) to postnatal day 14 (glomerulosa 37.8, fasciculata 37.3, reticularis 40.9/cell), as is shown in Fig. 41. The increase from embryo day 19 to postnatal day 14 was stochastically significant ($P < 0.01$).

3.2.1.1.1.2. Mitochondrial DNA synthesis

The results of visual grain counts on the number of mitochondria labeled with silver grains obtained from 10 adreno-cortical cells in the 3 layers of each animal labeled with ^{3}H-thymidine demonstrating DNA synthesis in 5 aging groups at perinatal stages, prenatal embryo day 19, postnatal day 1, 3, 9 and 14, are plotted in Fig. 42 (Ito & Nagata 1996). The results demonstrated that the numbers of labeled mitochondria with 3H-thymidine showing DNA synthesis gradually increased from prenatal embryo day 19 (glomerulosa 0.3, fasciculata 0.5, reticularis 0.4/cell) to postnatal day 14 (glomerulosa 1.5, fasciculata 1.5, reticularis 1.6/ cell), reaching the maximum.

3.2.1.1.1.3. The labeling index

On the other hand, the labeling indices in respective aging stages were calculated from the number of labeled mitochondria (Fig. 41) dividing by the number of total mitochondria per cell (Fig. 42) which were plotted in Fig. 43, respectively.

The results showed that the labeling indices gradually increased from prenatal day 19 (glomerulosa 2.4, fasciculata 2.7, reticularis 2.6%) to postnatal day 14 (glomerulosa 4.0, fasciculata 4.1, reticularis 3.9%), reaching the maximum (Fig. 43).

3.2.1.2. RNA synthesis in the adreno-cortical cells

In order to study the aging changes of intramitochondrial RNA synthesis of mouse adrenal cortical cells, 4 groups of aging mice, each consisting of 3 individuals, total 12, from postnatal newborn at day 14, adult at month 6 and senescent animals at month 12 (year 1) and 24 (year 2) were injected with ^{3}H-uridine, a RNA precursor, sacrificed 1 h later and the liver tissues were fixed, embedded in Epoxy resin, sectioned and processed for electron microscopic radioautography (Liang et al., 1999). On electron microscopic radioautograms obtained from each animal, the number of mitochondria per cell, the number of labeled mitochondria with ^{3}H-uridine showing RNA synthesis per cell and the mitochondrial labeling index in each adrenal cortical cells, in 3 zones, the zona glomerulasa, fasciculate and reticularis, were counted and the results in respective aging groups were compared with each others.

From the results, it was demonstrated that the number of mitochondria per cell in 3 zones of respective mice at various ages increased from postnatal day 14 to month 6 and 12, reaching the plateau from month 12 to 24 due to development and aging of animals, respectively, while the number of labeled mitochondria per cell and the labeling index of intramitochondrial RNA synthesis incorporating ^{3}H-uridine increased from postnatal day 14 to month 6 and 12, reaching the maxima and decreased from month 12 to month 24. It was shown that the activity of intramitochnodrial RNA synthesis in the adrenocortical cells in developing and aging mice changed due to aging of individual animals.

3.2.2. Adrenal medulla

3.2.2.1. The adreno-medullary cells

The adreno-medullary cells consist of 2 cell types, adrenalin cells and noradrenalin cells (Nagata, 2009c). From the results obtained at present, from aging ddY mice at various ages, it was concluded that almost all the cells, both adrenalin and noradrenalin cells, in the adrenal medullae of mice at various ages, from prenatal embryo day 19 to postnatal newborn, day 1, 3, 9 and 14, and to postnatal month 1, 2 and 6, were labeled with silver grains showing DNA synthesis with ^{3}H-thymidine in their mitochondria (Nagata, 2009c).

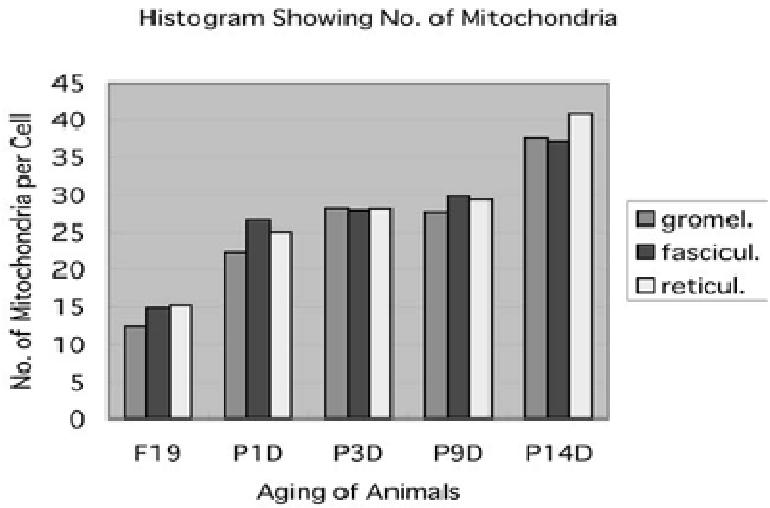

Figure 41: Histogram showing the aging changes of number of mitochondria per cell in 3 zones of glomerulosa, fasciculata and reticularis. It increased from embryo to postnatal day 14.

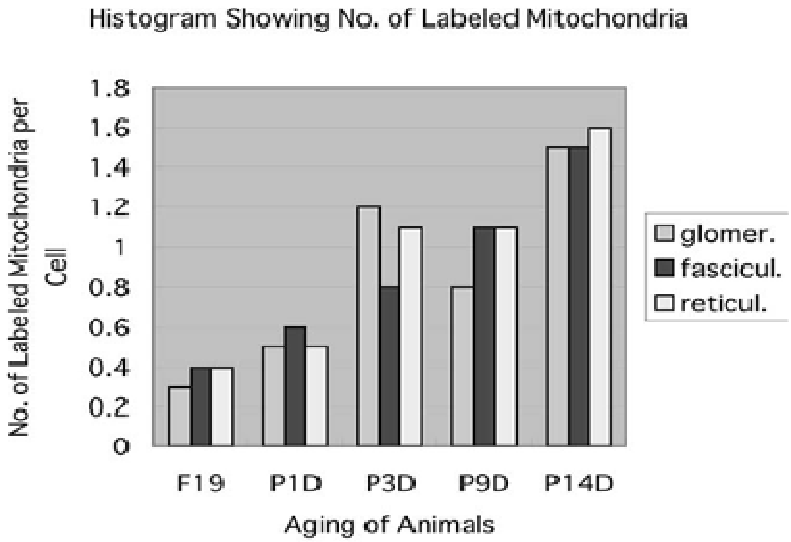

Figure 42: Histogram showing the aging changes of number of labeled mitochondria per cell in 3 zones of glomerulosa, fasciculata and reticularis. It increased from embryo to postnatal day 14.

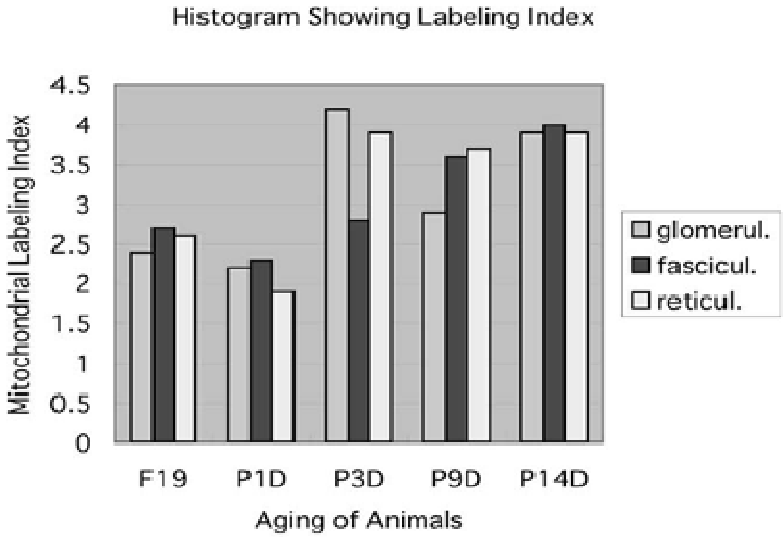

Figure 43: Histogram showing the aging changes of the labeling index of mitochondria in 3 zones of glomerulosa, fasciculata and reticularis. It increased from embryo to postnatal day 14.

3.2.2.2. Quantitative analysis on the number of mitochondria in adreno-medullary cells

The analysis resulted in increases from the prenatal day to postnatal day 1, 3, 9, 14, and month 1, 2 and 6, reaching the maximum at postnatal day 14 to month 6. To the contrary, the numbers of labeled mitochondria with ^{3}H-thymidine showing DNA synthesis and the labeling indices also increased from prenatal day 19 to postnatal day 14, reaching the maximum at postnatal day 14, and then decreased to month 1, 2 and 6. These results demonstrate that the number of mitochondria in adrenal cortical cells increased from perinatal stages to postnatal month 6 due to aging of animals, while the activity of mitochondrial DNA synthesis increased to postnatal day 14, due to development and de creased to month 6 to 2 years due to aging and senescence.

3.3. The Lung

The pulmonary tissues obtained from ddY strain mice at embryonic to early postnatal stages consisted of undifferentiated cells (Fig. 44). However, they differentiated into several types of cells due to aging, the type I epithelial cell (Fig. 45, 51) or the small alveolar epithelial cell, the type II epithelial cell (Fig. 46, 52) or the large alveolar epithelial cell, the interstitial cell (Fig. 47, 53), the endothelial cell and alveolar phagocyte or dust cell as we had formerly observed (Sun, 1995; Sun et al., 1994, 1995, 1997). At embryonic day 16 and 18, the fetal lung tissues appeared as glandular organizations consisting of many alveoli bordering undifferentiated cuboidal cells and no squamous epithelial cells were seen (Fig. 44). Mitotic figures were frequently observed in cuboidal epithelial cells. After birth, the structure of the alveoli was characterized by further development of the alveolar-capillary networks from postnatal day 1 to 3 and 7. During the development, the cellular composition of the alveolar epithelium resembled that of the adult lung, with a mixed population of the type I and type II epithelial cells. Up to 1 and 2 weeks after birth, the lung tissues showed complete alveolar structure and single capillary system almost the same as the adult after 1 month (Fig. 51, 52, 53) to 2 to 6 months, and further to senescent stage over 12 months to 24 months.

3.3.1. Light microscopic radioautography

We observed the thick sections (2.0µm), coated with LM radioautographic emulsion and found many undifferentiated cells were labeled in their nuclei synthesizing DNA at prenatal stages from embryo to newborn animals (Fig. 44).

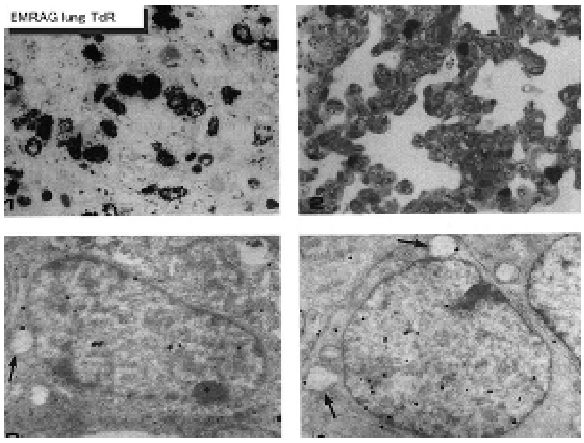

Figure 44: LMRAG of the lung tissues of mice at fetal day 16 (upper left), postnatal day 7 (upper right), and EMRAG of a mouse cuboidal cell at fetal day 16 (lower left), an interstitial cell (lower right).

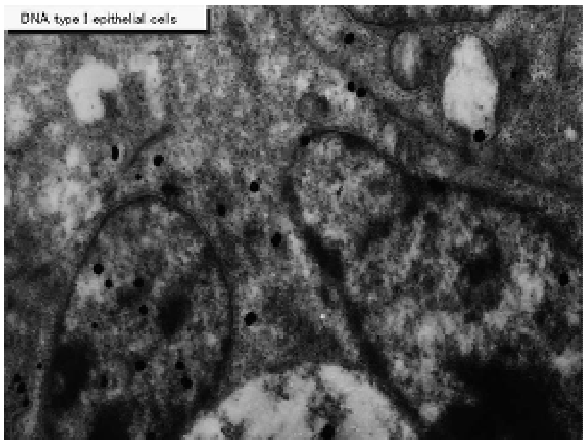

Figure 45: EMRAG of the type I epithelial cell of an adult mouse at postnatal month 1, labeled with 3H-thymidine. Silver grains are localized over nuclei and several mitochondria.

3.3.2. Electron microscopic radioautography

We observed the thin sections (0.2µm), coated with EM radioautographic emulsion and found silver grains appearing not only over their nuclei of the pulmonary cells but also over some mitochondria in the cytoplalsm synthesizing DNA (Figs. 45-47).

3.3.2.1. Mitochondrial DNA synthesis in the lung

On electron microscopic radioautograms of the pulmonary tissues labeled with ^{3}H-thymidine, silver grains were observed over the nuclei of some pulmonary cells corresponding to the DNA synthesis in S-phase as observed by light microscopic radioautograpy (Fig. 44). On the other hand, some mitochondria in both S-phase cells and interphase cells which did not show any silver grains over their nuclei were labeled with silver grains showing intramitochondrial DNA synthesis (Sun et al., 1995, 1997). The intramitochondrial DNA synthesis was observed in all the cell types, the type I epithelial cell (Fig. 45, 51), the type II epithelial cell (Fig. 46, 52), the interstitial cell (Fig. 47, 53) and the endothelial cell. Because enough numbers of electron photographs (more than 5) were not obtained from all the cell types in respective aging groups, only some cell types and some aging groups where enough numbers of electron photographs were available were used for quantitative analysis. The numbers of mitochondria per cell profile area, the numbers of labeled mitochondria per cell and the labeling indices of the type I epithelial cells in only a few aging groups was shown in Fig. 48 (top). Likewise, the similar results from the type II epithelial cells (Fig. 49 top), the interstitial cells (Fig. 50 top) were shown. The labeling indices in respective aging stages were calculated from the number of labeled mitochondria and the number of total mitochondria per cellular profile area which were plotted in Figs. 48, 49, 50 (middle and bottom), respectively. These results demonstrated that the labeling indices in these cell types decreased from perinatal stages to the adult and senescent stage due to aging.

3.3.2.2. Mitochondrial RNA synthesis in the lung

On electron microscopic radioautograms of pulmonary tissues labeled with ^{3}H-uridine, silver grains were observed over the nuclei of some pulmonary cells corresponding to the RNA synthesis in most cells in respective aging groups as observed by light microscopic radioautograpy (Sun, 1995). The silver grains were observed to localize not only over euchromatin and nucleoli in the nuclei but also over many cell organelles such as endoplasmic reticulum, ribosomes, and mitochondria as well as cytoplasmic matrices of all the cell types (Sun, 1995). The intramitochondrial RNA synthesis was observed in all the cell types, the interstitial cell (Fig. 51) the type I epithelial cell (Fig. 52), the type II epithelial cell (Fig. 53), and the endothelial cell. Because enough numbers of electron photographs (more than 5) were not obtained from all the cell types in respective aging groups, only some cell types and some aging groups when enough numbers of electron photographs were available were used for quantitative analysis similarly to DNA

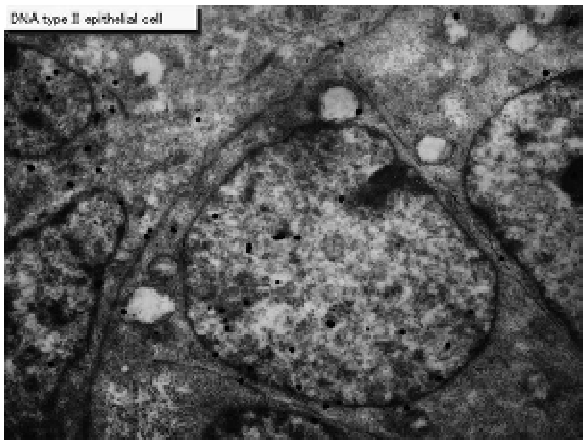

Figure 46: EMRAG of the type II epithelial cell of an adult mouse at postnatal month 1, labeled with 3H-thymidine. Silver grains are localized over

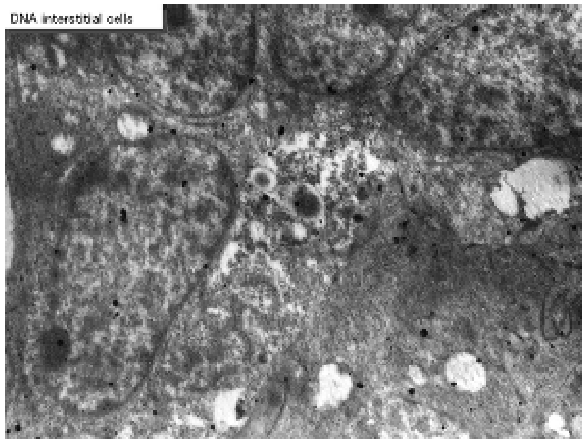

Figure 47: EMRAG of the interstitial cell of an adult mouse at postnatal month 1, labeled with 3H-thymidine. Silver grains are localized over nuclei

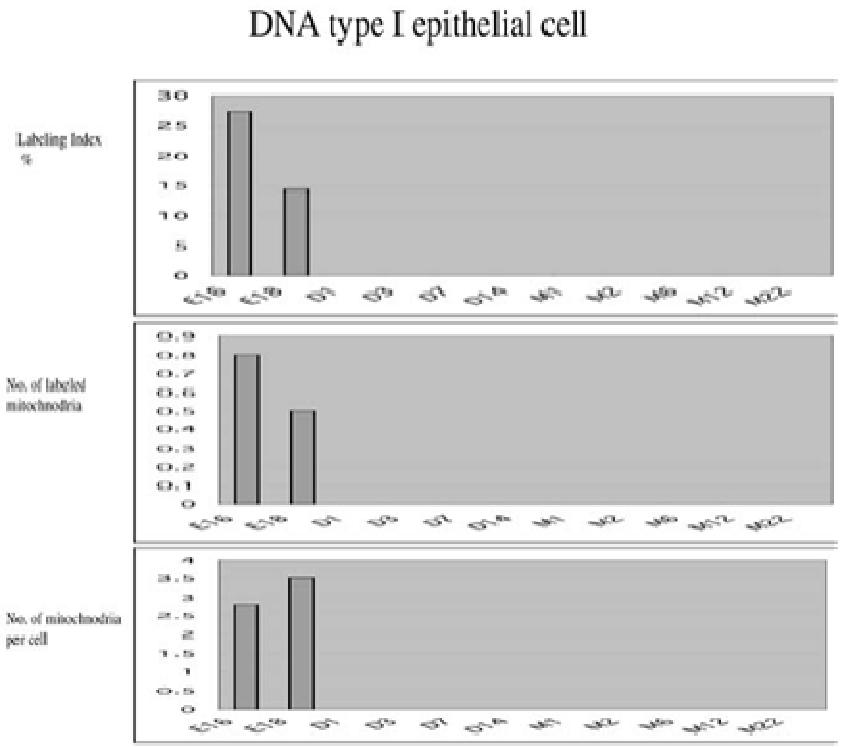

Figure 48: Histograms demonstrating the labeling index (top), number of labeled mitochondria (middle) and number of mitochondria (bottom) of the type I epithelial cells labeled with 3H-thymidine.

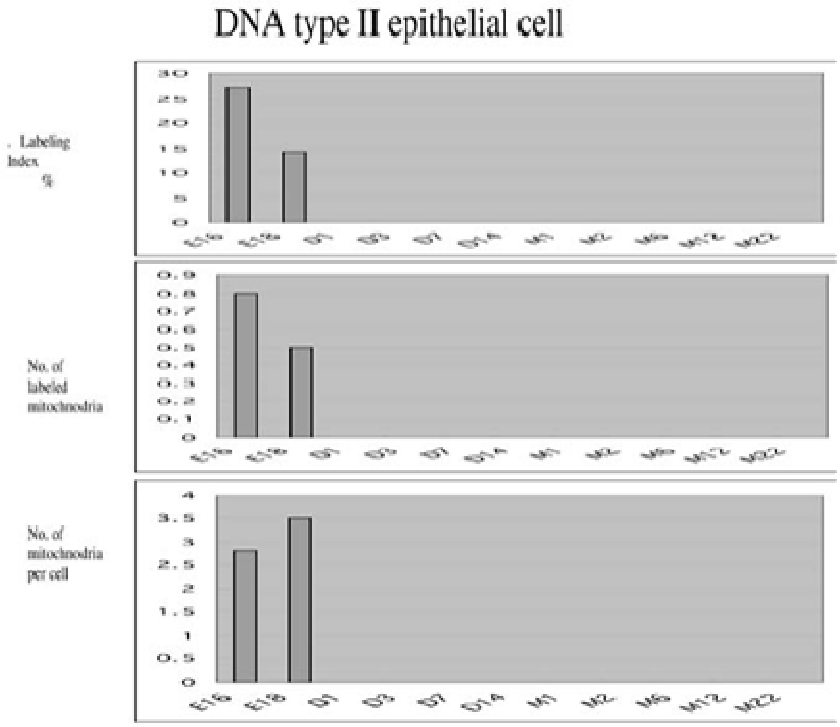

Figure 49: Histograms demonstrating the labeling index (top), number of labeled mitochondria (middle) and number of mitochondria (bottom) of the type II epithelial cells labeled with 3H-thymidine.

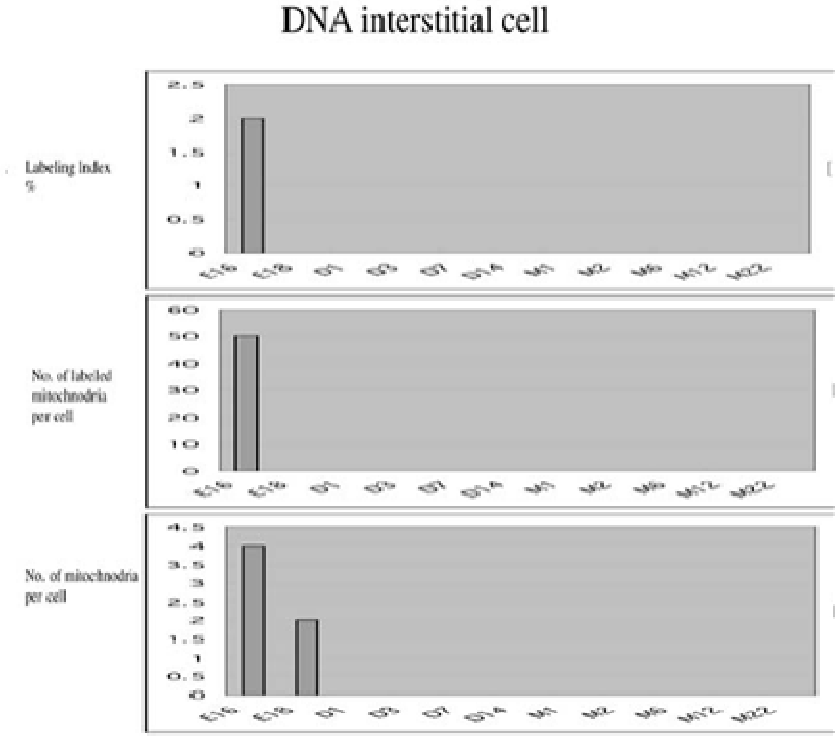

Figure 50: Histograms demonstrating the labeling index (top), number of labeled mitochondria (middle) and number of mitochondria (bottom) of the interstitial cells labeled with 3H-thymidine.

synthesis. The numbers of mitochondria per cell profile area, the numbers of labeled mitochondria per cell and the labeling indices of the type I epithelial cells in only a few aging groups was shown in Fig. 54. Likewise, the similar results from the type II epithelial cells (Fig. 55 bottom), the interstitial cells (Fig. 56 bottom), and the endothelial cell (Fig. 57 bottom) were shown. The labeling indices in respective aging stages were calculated from the number of labeled mitochondria and the number of total mitochondria per cellular profile area were also shown in Figs. 54-57 (top and middle), respectively. These results demonstrated that the numbers of labeled mitochondria in these cell types increased from perinatal stages to the adult stage, reaching maxima at postnatal month 1, and decreased to the senescent stage due to aging.

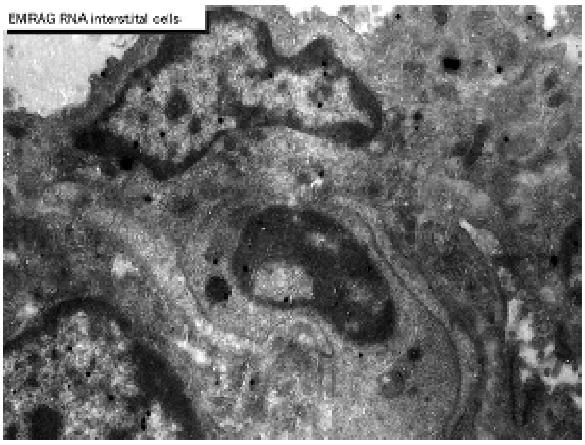

Figure 51: EMRAG of the interstitial cell of an adult mouse at postnatal month 1, labeled with 3H-uridine. Silver grains are localized over nucleus and several mitochondria.

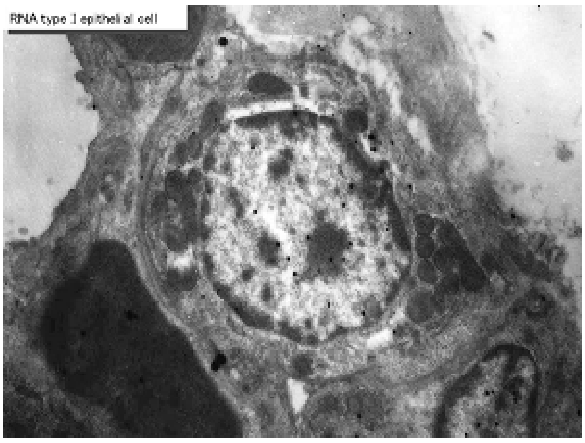

Figure 52: EMRAG of the type I epithelial cell of an adult mouse at postnatal month 1, labeled with 3H-uridine. Silver grains are localized over nucleus and several mitochondria.

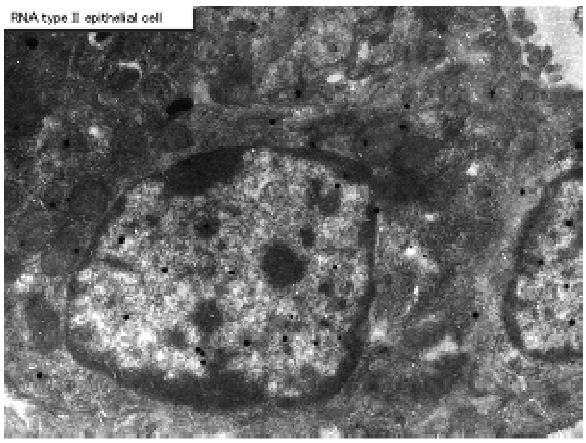

Figure 53: EMRAG of the type II epithelial cell of an adult mouse at postnatal month 1, labeled with 3H-uridine. Silver grains are localized over nucleus and several mitochondria.

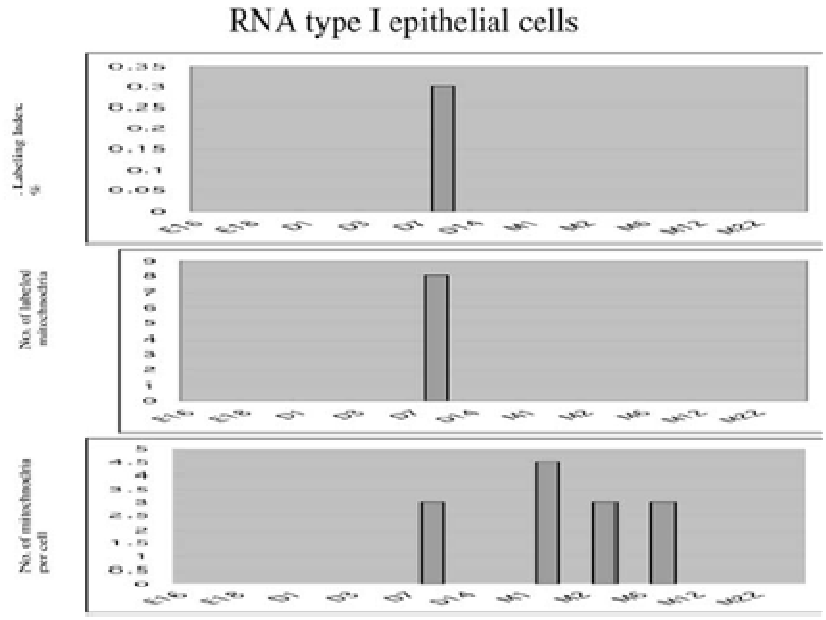

Figure 54: Histograms demonstrating the labeling index (top), number of labeled mitochondria (middle) and number of mitochondria (bottom) of the type I epithelial cell of an adult mouse at postnatal month 1, labeled with ^{3}H-uridine.

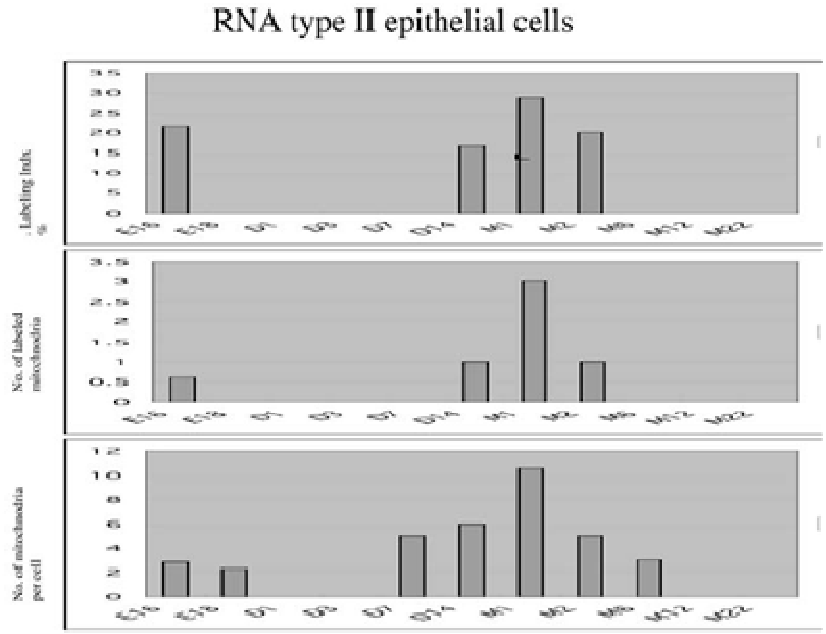

Figure 55: Histograms demonstrating the labeling index (top), number of labeled mitochondria (middle) and number of mitochondria (bottom) of the type II epithelial cells labeled with ^{3}H-uridine.

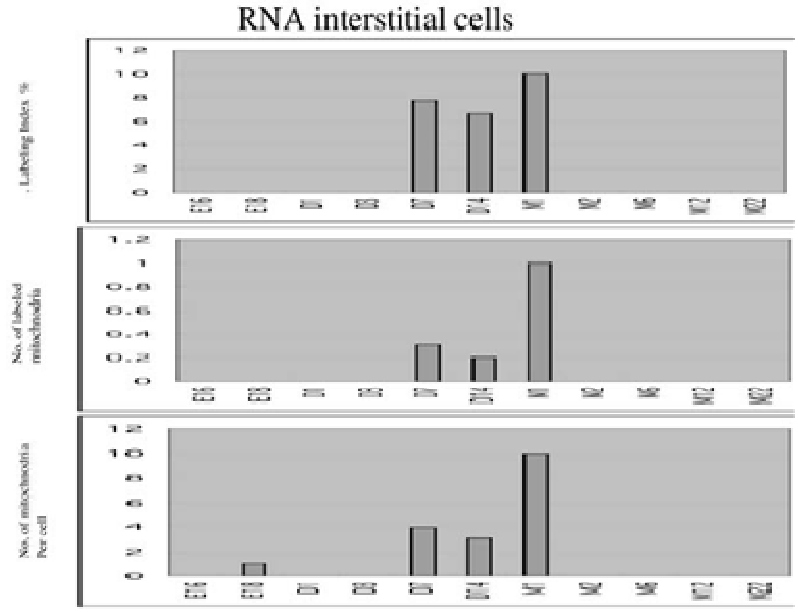

Figure 56: Histograms demonstrating the labeling index (top), number of labeled mitochondria (middle) and number of mitochondria (bottom) of the interstitial cells labeled with ^{3}H-uridine.

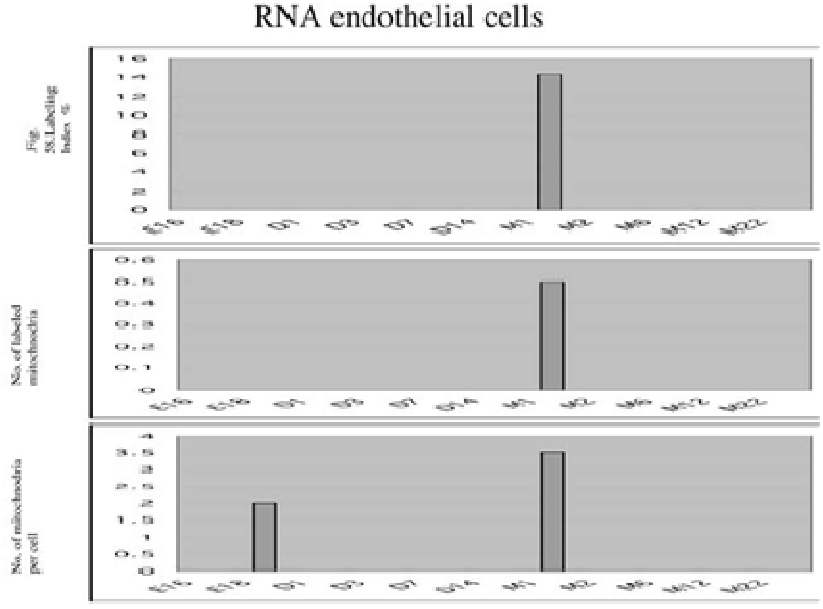

Figure 57: Histograms demonstrating the labeling index (top), number of labeled mitochondria (middle) and number of mitochondria (bottom) of the endothelial cells labeled with ^{3}H-uridine.

3.4. The testis

The male reproductive system of a ddY mouse consists of the testis and its excretory ducts. We studied the macromolecular synthesis in the testis of aging ddY mice at various ages (Gao et al., 1994, 1995) . By LM and EM radioautography, many spermatogonia and myoid cells were labeled with 3H-thymidine at various ages from embryonic day 19 to postnatal day 1, 4, 7, 14 (Fig. 58), month 1, 2, 6, 9, 12 and 24. Silver grains are localized over the nuclei and several mitochondria of the spermatogonia showing DNA synthesis. Among of the aging groups, we calculated the numbers of mitochondria per cell profile area, the numbers of labeled mitochondria per cell and the labeling indices of the spermatogonia from 4 aging groups, prenatal embryonic day 19, postnatal day 4, month 1 and 6. The results were listed in Table 1. It is clear that the LI of the spermatogonia increased from embryonic day 19 to postnatal month 1 (day 30), reaching the maximum, then decreased to month 6.

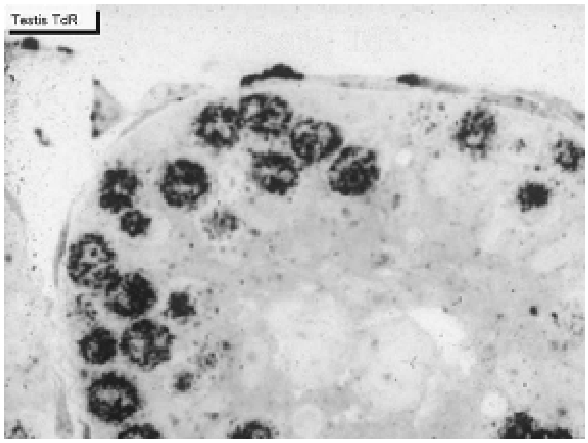

Fig 58: LM RAG of a young mouse testis at postnatal day 14 labeled with 3H-thymidine, showing many spermatogonia and myoid cells which were labeled with silver grains in the nuclei demonstrating DNA synthesis.

Table 1: Labeling index of spermatogonia mitochondria in mouse testis labeled with ^{3}H-thymidine.

Age	Labeling Index of Mitochondria
Prenatal day 19	17.0%
Postnatal day 4	12.6%
Postnatal month 1	30.5%
Postnatal month 6	26.0%

3.5. Other organs

At present, several other organs such as the pancreas and the kidney are under examination and the results shall be shown elsewhere in the future.

4. Concluding Remarks

From the results obtained at present, nucleic acids, both DNA and RNA, and protein synthesis showing incorporations of ^{3}H-thymidine, ^{3}H-uridine and ^{3}H-leucine were demonstrated in the nuclei and mitochondria of hepatocytes of the liver, adreno-cortical and medullary cells of the adrenal glands, 4 types of pulmonary cells of the lung and spermatogonia of mice at various ages from fetal to postnatal newborn, juvenile, young, adult and senescence.

The numbers of mitochondria per cell, the numbers of labeled mitochondria and the labeling indices of hepatocytes, adreno-cortical and medullary cells, pulmonary cells and spermatogonia at various ages changed due to aging, increases and decreases, independent from the nuclei.

We have also studied macromolecular synthesis of mitochondria in other cell types *in vivo* since we had found DNA, RNA and protein syntheses in cultured cells *in vitro* (Nagata et al., 1967). The results were reviewed in previous review article (Nagata, 2002), as well as in several recent monographs (Nagata, 2007, 2008;, 2009).

These results indicate that the mitochondria in respective cell types of these organs synthesize DNA, RNA and proteins by themselves, increase and decrease due to the aging of the individual animals.

On the other hand, these results form parts of special cytochemistry (Nagata, 2001) and special radioautographology (Nagata, 2002) as the present author formerly proposed.

5. Acknowledgements

The most parts of the studies concerning to the livers and the adrenal glands of aging mice was supported by Grant-in-Aids for Scientific Research from the Japan Society for Promotion of Sciences (No. 18924034, No. 19924204 and No. 20929003) while the author has been working at Shinshu Institute of Alternative Medicine and Welfare since 2005 up to the present time as Professor of Anatomy after retirement from Shinshu University. The author is also grateful to Grant-in-Aids for Scientific Research from the Ministry of Education, Science and Culture of Japan (No. 02454564) while the author worked at Department of Anatomy and Cell Biology as Professor and Chair, Shinshu University School of Medicine (from 1974 to1996), as well as Grants for Promotion of Characteristic Research and Education from the Japan Foundation for Promotion of Private Schools (1997, 1998 1999, 2000) while the author worked at Nagano Women's Jr. College as Professor of Anatomy. The author thanks Dr. Kiyokazu Kametani, Technical Official, Department of Instrumental Analysis, Research Center for Human and Environmental Sciences, Shinshu University, for his technical assistance during the course of this study.

6. References

Cui H, Gao F, Ma H, Nagata T. Study on DNA synthesis of cellular elements in the cerebella of aging mice by light and electron microscopic radioautography. Proc 4th China-Japan Joint Histochem Cytochem Symp, Chongqing Publishing House, Chongqing, 1996;4:111-2.

Gao F, Chen S, Sun L, Kang W, Wang Z, Nagata T. Radioautographic study of the macromolecular synthesis of Leydig cells in aging mouse testis. Cell Mol Biol 1995;41:145-50.

Gao F, Ma H, Sun L, Jin C, Nagata T. Electron microscopic radioautographic study on the nucleic acid and protein synthesis in the aging mouse testis. Med Electron Microsc 1994;27:360-2.

Gunarso W, Gao F, Cui H, Ma H, Nagata T. A light and electron microscopic radioautographic study on RNA synthesis in the retina of chick embryo. Acta Histochem. 1996;98:300-22.

Gunarso W, Gao F; Nagata, T.: Development and DNA synthesis in the retina of chick embryo observed by light and electron microscopic radioautography. Cell Mol Biol. 1997;43:189-201.

Hanai T, Nagata T. Electron microscopic radioautographic study on nucleic acid synthesis in perinatal mouse kidney tissue. Med Electron Microsc 1994;27:355-7.

Ito M, Nagata T. Electron microscopic radioautographic study on DNA synthesis and the ultrastructure of the adrenal gland in aging mice. Med Electron Microsc 1996;29:145-52.

Kong Y, Nagata T. Electron microscopic radioautographic study on nucleic acid synthesis of perinatal mouse retina. Med Electron Microsc 1994;27:366-8.

Ma H, Gao F, Sun L, Jin C, Nagata T. Electron microscopic radioautographic study on the synthesis of DNA, RNA and protein in the livers of aging mice. Med Electron Microsc 1994;27:349-51.
Ma H, Nagata T. Studies on DNA synthesis of aging mice by means of electron microscopic radioautography. J Clin Electron Microsc 1988;21:335-43.
Nagata T. Radioautographic study on intramitochondrial nucleic acid synthesis: Its relationship to the cell cycle in cultivated cells. Proc 4th Internat Cong Histochem Cytochem, Jap Soc Histochem Cytochem, ed, Kyoto, 1972a;4:223-4.
Nagata T. Electron microscopic radioautography of intramitochondrial RNA synthesis of HeLa cells in culture. Histochemie 1972b;32:163-70.
Nagata T. Quantitative electron microscope radioautography of intramitochondrial nucleic acid synthesis. Acta Histochem Cytochem 1972c; 5: 201-203.
Nagata T. Electron microscopic radioautography of intramitochondrial nucleic acid syntheses in mammalian cells in vitro. Proc 8th Internat Cong Electron Microsc, Australia Electron Microsc Soc, ed, Canberra, 1974;II:346-7.
Nagata T. Electron microscopic observation of target cells previously observed by phase-contrast microscopy: Electron microscopic radioautography of laser beam irradiated cultured cells. J Clin Electron Microsc 1984;17:589-590.
Nagata T. Radiolabeling of soluble and insoluble compounds as demonstrated by light and electron microscopy. In: Wegmann R J, Wegmann M A (editors). Recent Advances in Cellular and Molecular Biology. Leuven: Peters Press, 1992;6:9-21.
Nagata T. Techniques and application of electron microscopic radioautography. J Electron Microsc 1996;45:258-74.
Nagata T. Techniques and application of microscopic radioautography. Histol Histopathol 1997;12:1091-124.
Nagata T. Special Cytochemistry in Cell Biology. In: Jeon KW (ed). Internat Rev Cytol. New York: Academic Press, 2001;211:33-151.
Nagata T. Radioautographology, General and Special. Prog Histochem Cytochem, Graumann W ed, Urban & Fischer, Jena 2002;37(2):57-226.
Nagata T. Electron microscopic radioautographic study on protein synthesis in hepatocyte mitochondria of developing mice. Ann Microsc 2006;6:43-54.
Nagata T. Electron microscopic radioautographic study on macromolecular synthesis in hepatocyte mitochondria of aging mouse. J Cell Tis Res 2007a; 7:1019-29.
Nagata T. Electron microscopic radioautographic study on nucleic acids synthesis in hepatocyte mitochondria of developing mice. Trends Cell Mol Biol 2007b;2: 9-33.
Nagata T. Electron microscopic radioautographic study on protein synthesis in mitochondria of binucleate hepatocytes in aging mice. Sci World J 2007c; 7: 1008-23.
Nagata T. Aging changes of macromolecular synthesis in the mitochondria of mouse hepatocytes as revealed by microscopic radioautography. Annu Rev Biomed Sci 2007d;9:30-6.
Nagata T. Macromolecular synthesis in hepatocyte mitochondria of aging mice as revealed by electron microscopic radioautography. I. Nucleic acid synthesis. In: Vilas AM, Alvarez JD (editors). Modern Research and Educational Topics in Microscopy. Badajoz, Spain: Formatex, 2007e; 1:245-58.
Nagata T. Macromolecular synthesis in hepatocyte mitochondria of aging mice as revealed by electron microscopic radioautography. II. Protein synthesis. In: Vilas AM, Alvarez JD (editors). Modern Research and Educational Topics in Microscopy. Badajoz, Spain: Formatex,, 2007f; Vol. 1: pp. 259-271.
Nagata T.: Sexual difference between the macromolecular synthesis of hepatocyte mitochondria in male and female mice in aging as revealed by electron microscopic radioautography. Chapter 22. In: Benninghouse HT, Rosset AG, (editors). Women and Aging. USA: Nova Sci Publishers, 2008:461-87.
Nagata T. Protein synthesis in hepatocytes of mice as revealed by electron microscopic radioautography. In: Esterhouse TE, Petrinos LB (editors), Protein Biosynthesis. New York: Nova Sci Publishers, 2009a;133-61.
Nagata T. Recent studies on macromolecular synthesis labeled with ^{3}H-thymidine in various organs as revealed by electron microscopic radioautography. Current Radiopharmaceutics 2009b;2:118-28.
Nagata T. Electron microscopic radioautographic study on mitochoindrial DNA synthesis in adrenal medullary cells of developing and aging mice. J Cell Tis Res 2009c;9:1793-802.

Nagata T, Fujii Y, Usuda N. Demonstration of extranuclear nucleic acid synthesis in mammalian cells under experimental conditions by electron microscopic radioautography. Proc 10th Internat Cong Electron Microsc, Hamburg 1982;2:305-6.
Nagata T, Ito M, Chen S. Aging changes of DNA synthesis in the submandibular glands of mice as observed by light and electron microscopic radioautography. Ann Microsc 2000;1:13-22.
Nagata T, Iwadare N, Murata F. Electron microscopic radioautography of nucleic acid synthesis in cultured cells treated with several carcinogens. Acta Pharmacol Toxicol 1977;41:64-5.
Nagata T, Ma H. Electron microscopic radioautographic study on nucleic acid synthesis in amitotic hepatocytes of the aging mouse. Med Electron Microsc 2003;36:263-71.
Nagata T, Ma H. Electron microscopic radioautographic study on mitochondrial DNA synthesis in hepatocytes of aging mouse. Ann Microsc 2005a;5:4-18.
Nagata T, Ma H. Electron microscopic radioautographic study on RNA synthesis in hepatocytes of aging mouse. Microsc Res Tech 2005b;64:55-64.
Nagata T, Ma H. Electron microscopic radioautographic study of RNA synthesis in hepatocyte mitochondria of aging mouse. Microsc Res Tech 2005c;67:55-64.
Nagata T, Murata F. Electron microscopic dry-mounting radioautography for diffusible compounds by means of ultracryotomy. Histochemistry 1977;54:75-82.
Nagata T, Ohno S, Kawahara I, Yamabayashi S, Fujii Y, Murata F. Light and electron microscopic radioautography of nucleic acid synthesis in mitochondria and peroxisomes of rat hepatic cells during and after DEHP administration. Acta Histochem Cytochem 1979;16:610-1.
Nagata T, Ohno S, Yoshida K, Murata F. Nucleic acid synthesis in proliferating peroxisomes of rat liver as revealed by electron microscopical radioautography. Histochem J 1982;14:197-204.
Nagata T, Shibata O, Nawa T. Incorporation of tritiated thymidine into mitochondrial DNA of the liver and kidney cells of chickens and mice in tissue culture. Histochemie 1967;10:305-8.
Nagata T, Usuda N, Ma H. Electron microscopic radioautography of nucleic acid synthesis in pancreatic acinar cells of prenatal and postnatal aging mice. Proc 11th Internat Cong Electron Microsc, Kyoto 1986;3:2281-2.
Nagata T, Yamada Y, Iwadare N, Murata F. Relationship of intramitochondrial nucleic acid synthesis to the nucleoli in cultivated cells as revealed by electron microscopic radioautography. Proc 10th Internat Cong Anat, Jap Assoc Anat, ed, Tokyo 1975;474-5.
Sun L. Age related changes of RNA synthesis in the lungs of aging mice by light and electron microscopic radioautography. Cell Mol Biol 1995;41:1061-72.
Sun L, Gao F, Jin C, Nagata T. DNA synthesis in the trachea of aging mice by light and electron microscopic radioautography. Acta Histochem Cytochem 1997;30:211-20.
Sun L, Gao F, Nagata T. Study on the DNA synthesis of pulmonary cells in aging mice by light microscopic radioautography. Cell Mol Biol 1995;41:851-9.
Yamada A T, Nagata T. Light and electron microscopic radioautography of DNA synthesis in the endometria of pregnant ovariectomized mice during activation of implantation window. Cell Mol Biol 1994a;38:763-74.
Yamada A T, Nagata T. Ribonucleic acid and protein synthesis in the uterus of pregnant mouse during activation of implantation window. Med Electron Microsc 1994b;27:363-5.